The Role of eIF4G-1 Isoforms and Live Cell Imaging of IRES-mediated Translation Initiation in Breast Cancer Cells

By

Whitney K. Crosson

Dr. Brett D. Keiper and Dr. Mary A. Farwell
Thesis Advisors

Department of Biology
East Carolina University

The development of cancer is a consequence of mutations that lead to dysfunctional cell processes such as unrestrained cell proliferation, resistance to apoptosis, and improper regulation of cell processes such as translation. Cell proliferation and apoptosis are linked to specific gene expression events regulated by protein synthesis, which begins with the binding of various eukaryotic initiation factors (eIF) to mRNA and ribosomes to initiate translation. eIF4G-1 catalyzes two types of translation initiation. Cap-dependent translation requires eIF4E to bind a 5'-methylated mRNA cap and eIF4G-1. This in turn facilitates recruitment and promotes translation of cell cycle and growth-related proteins. Cap-independent translation initiates internally through internal ribosome entry sites (IRES) in the 5' UTR of mRNA and promotes translation of apoptotic mRNAs such as Apaf-1. Previous studies found that eight variants of eIF4G-1 mRNA exist, and five protein isoforms can be resolved by electrophoresis. Each isoform may potentially form a translation complex with activities that differ slightly based on modular binding sites. We hypothesized that the representation of eIF4G-1 isoforms and their activity in the initiation complex varies in tumor-forming human breast cell lines vs. non-tumor-forming lines. However, when eIF4G-1 isoform representation was determined in three breast carcinoma cell lines and one non-tumorigenic breast epithelium cell line, no such systematic increase or decrease of individual isoforms was found. Similar results were seen after two breast

cancer cell lines were treated with the chemotherapeutic reagents etoposide and cisplatin. Previous studies in our laboratory demonstrated that in population of human breast cancer cells cap-independent translation could be induced as indicated by the use Apaf-1 IRES, suggesting a shift towards pro-apoptotic protein synthesis. We have now developed a novel dual fluorescence bicistronic reporter containing either the Apaf-1 IRES, or a viral IRES to assay the propensity of these cells on an individual cell basis toward cap-independent translation in vivo. Our results confirm the ability of this assay to measure the ratio of cap-dependent versus cap-independent initiation in single live cells as demonstrated by blue fluorescence or green fluorescence, respectively. By establishing the role of eIF4G-1 isoforms in pro-apoptotic protein synthesis, it may be possible to direct a cell from proliferation to apoptosis by targeting certain isoforms.

The Role of eIF4G-1 Isoforms and Live Cell Imaging of IRES-mediated Translation Initiation in Breast Cancer Cells

A Thesis

Presented to the Faculty of the Department of Biology

East Carolina University

In Partial Fulfillment for the Requirements for the Degree

Master of Science in Molecular Biology and Biotechnology

By

Whitney K. Crosson

April, 2012

The Role of eIF4G-1 Isoforms and Live Cell Imaging of IRES-mediated Translation Initiation in Breast Cancer Cells

By

Whitney K. Crosson

Approved By:

Co-Director of Thesis: _____
Brett D. Keiper, Ph.D.

Co-Director of Thesis: _____
Mary A. Farwell, Ph.D.

Committee Member: _____
Jean-Luc Scemama, Ph.D.

Committee Member: _____
Kathryn Verbanac, Ph.D.

Chair of the Department of Biology:

_____
Jeff McKinnon, Ph.D.

Dean of the Graduate School:

_____
Paul J. Gemperline, Ph.D.

ACKNOWLEDGEMENTS

I would like to thank Dr. Mary Farwell and Dr. Brett Keiper for accepting me into their labs and giving me the opportunity to work on this project. I would like to thank Dr. Keiper specifically for teaching me the value of a ‘chalk talk’ and making me do math in my head even though I hate it. ☺

I would also like to thank my committee members Dr. Jean-Luc Scemama and Dr. Kathryn Verbanac for their time and guidance, particularly in cell culture, over the course of my project. I would also like to thank the Brody School of Medicine Biochemistry Department for taking me in as one of their own.

TABLE OF CONTENTS:

LIST OF TABLES:

LIST OF FIGURES:

Introduction

Breast cancer continues to be a major health issue among women, accounting for 28% of all newly diagnosed cancer cases in 2010 (Jemal, Siegel et al. 2010). Cancer is a disease that can be attributed to mutations that cause unregulated cell proliferation, resistance to apoptosis, and prolonged cell survival. Mutations in genes that act as proto-oncogenes or tumor suppressors are responsible for the bulk of cancer development (Vermeulen, Van Bockstaele et al. 2003). Under normal conditions, proto-oncogenes stimulate regulated proliferation, but if dysfunction occurs can promote unrestrained cell growth. Tumor suppressor genes generally act as cell cycle regulators to suppress uncontrolled growth. When loss-of-function mutations occur, proliferation can continue unchecked. Over-expression of proto-oncogenes such as c-Myc, and mutations in tumor supressors, such as p53, allow a bypass in crucial cell cycle checkpoints, as well as an increase in proliferation, which necessitates an increase in protein synthesis to maintain growth requirements for the increased cell number and mass (Evan and Vousden 2001).

Breast cancer progresses through five major stages, with two main types of invasive carcinomas: ductal carcinoma and lobular carcinoma. Lobular carcinoma can be characterized by abnormal cells in the milk-producing lobules of the breast, whereas abnormal cells found in the ducts, which carry milk to the nipples, define ductal carcinoma. Breast cancer stages range from the mere presence of abnormal, non-invasive cells confined to the breast (Stage 0) to the metastasis of the cancer to other organs, most commonly the bones, lung, liver, and brain (Stage 4). Increasing tumor size, either by itself or combined with metastasis of the cancer to lymph nodes or distant sites, corresponds with a higher stage of breast cancer (NCI, 2009).

There are a variety of factors that contribute to the risk of developing breast cancer such as gene mutations and family history. Mutations in the Breast Cancer susceptibility genes 1 & 2 (BRCA1, BRCA2), which act as tumor suppressors, put an individual at a high risk of developing breast cancer in their lifetime. If there is a previous history of breast cancer within a family, then the age of onset of the cancer, the degree of the relationship to the individual with cancer, and the number of cases within a family are all taken into consideration when determining an individual's risk for breast cancer. Other risk factors include hormonal risks, such as a prolonged exposure to endogenous or exogenous estrogens, as well as lifestyle risks such as diet and exercise (Evans and Howell 2007).

Current treatments for breast cancer include surgery, chemotherapy, radiation therapy; all of which are commonly used in conjunction with molecular targeted therapies. A well known form of molecular targeted therapy is the use of drugs to manipulate receptors such as tamoxifen and trastuzumab. Tamoxifen works through competitive inhibition of estrogen receptors, which inhibits expression of estrogen induced genes, like growth factors, as well as some angiogenic factors that are secreted by the tumor (Osborne 1998). Human epidermal growth factor receptor (EGFR) 2 (HER2, or HER2/neu) is amplified in 25-30% of breast cancers, and overexpression is correlated to a decreased overall survival rate of the patient. Trastuzumab is a monoclonal antibody which recognizes the HER2 receptor $p185^{HER2}$, and works to block EGF-mediated proliferation (Vogel, Cobleigh et al. 2002).

Even though these treatments have an overall effectiveness towards reducing the cancer, there is still the issue of intrinsic or acquired resistance, and their specificity to a particular molecular pathway. In order to increase effectiveness of treatment, new targeted therapies that

focus on cell cycle progression, signal transduction, and the induction of apoptosis are being investigated (Schlotter, Vogt et al. 2008). An example of the latter targeted therapy is the manipulation of the apoptotic protein Bcl-2. Under normal cellular conditions Bcl-2 acts as a suppressor of apoptosis, but when overexpressed can lead to oncogenesis. Overexpression of Bcl-2 is seen in up to 80% of breast cancer cases, and has been associated with the resistance of tumor cells to cytotoxic drugs (Schlotter, Vogt et al. 2008). In order to counteract this effect, studies targeting Bcl-2 mRNA are taking place. In 2008, phase 1 clinical trials were in progress testing the downregulation of Bcl-2 mRNA translation using phosphorothioate antisense oligodeoxynuclotides (Schlotter, Vogt et al. 2008). While suppression of protein synthesis for a specific anti-apoptotic protein is already being attempted, an alternate approach to this type of molecular therapy is to investigate if a distinct mode of protein synthesis produces pro-apoptotic proteins within breast cancer cells. This approach is being explored through the project described in this thesis. The potential killing of cancer cells by promoting apoptotic protein synthesis is the long-term aim of this project.

The regulated formation of the translation initiation complex in eukaryotes plays a critical role in protein synthesis. (Vogel, Cobleigh et al. 2002) more specifically, the recruitment of eukaryotic initiation factors eIF4G (4G) and eIF4E to the complex. eIF4G is responsible for the coordination of all the factors and exists in multiple isoforms (Keiper, Gan et al. 1999; Byrd, Zamora et al. 2002). Understanding the role the various isoforms of eIF4G-1 may give insight to the regulation of protein synthesis in cancerous cells.

Hypothesis

In human breast cancer cell lines of varying aggressiveness, the representation eIF4G isoforms will vary, as will the predominant mode of translation initiation mechanism being used. Complexes of eIF4 that utilize eIF4G-I and eIF4G-II promote cap-dependent translation initiation and therefore facilitate cell proliferation through the increased translation of growth factors. Initiation complexes that utilize p97 or cleaved eIF4G-I promote cap-independent translation and therefore apoptosis through increased translation of apoptotic proteins. Exploration of this hypothesis breaks down into three components:

1. The many isoforms of eIF4G-I will themselves be represented differently in aggressive, tumor-forming human breast cell lines vs. non-tumor-forming lines.
2. The relative cap-dependent and –independent activities (as measured by the activities of viral and apoptotic Internal Ribosome Entry Sites (IRESes)) will be represented differently in aggressive, tumor-forming breast cell lines vs. non-tumor-forming lines.
3. The relative levels of cap-dependent to –independent activities will change upon treatment using an apoptotic agent like etoposide or cis-platin by enhancing cap-independent pro-apoptotic IRESes.

Background

Eukaryotic Translation Initiation Complex

Translation initiation can occur by at least two mechanisms; cap-dependent initiation and cap-independent initiation (Figure 1). Eukaryotic initiation factor 4G (eIF4G), the central scaffold protein, binds eIF4E (4E), an mRNA cap binding subunit, and eIF4A (4A), a mRNA helicase. Together they form the complex eIF4F, and facilitate the binding of the 40S ribosomal subunit to the mRNA to form the 48S complex(Keiper, Gan et al. 1999; Prevot, Darlix et al. 2003). eIF4G also interacts with the poly A binding protein (PABP), which binds the 3' poly A tail of mRNA to the initiation complex, increasing efficiency of translation by circularizing the mRNA and allowing increased recycling of the associated ribosomes (Keiper and Rhoads 1997). The 5' end of eukaryotic mRNA contains a 7-methylguanosine triphosphate cap which binds eIF4E, the cap binding protein. Cap-dependent translation initiation refers to the requirement of eIF4G to bind the cap binding protein, thus the mode of translation is dependent upon 5' mRNA cap association. By contrast, cap-independent translation does not rely on 5' cap association nor eIF4E. During cap-independent translation, eIF4G-1 is often proteolytically cleaved into two portions; the N-Terminal domain (cp_n) and the C-Terminal domain (cp_c) (Keiper, Gan et al. 1999). This cleavage causes eIF4G to release the cap binding protein eIF4E and PABP. Translation still able to occurs through internal ribosome entry sites (IRES) which direct the placement of ribosomes to internal AUG start sites.

Figure 1

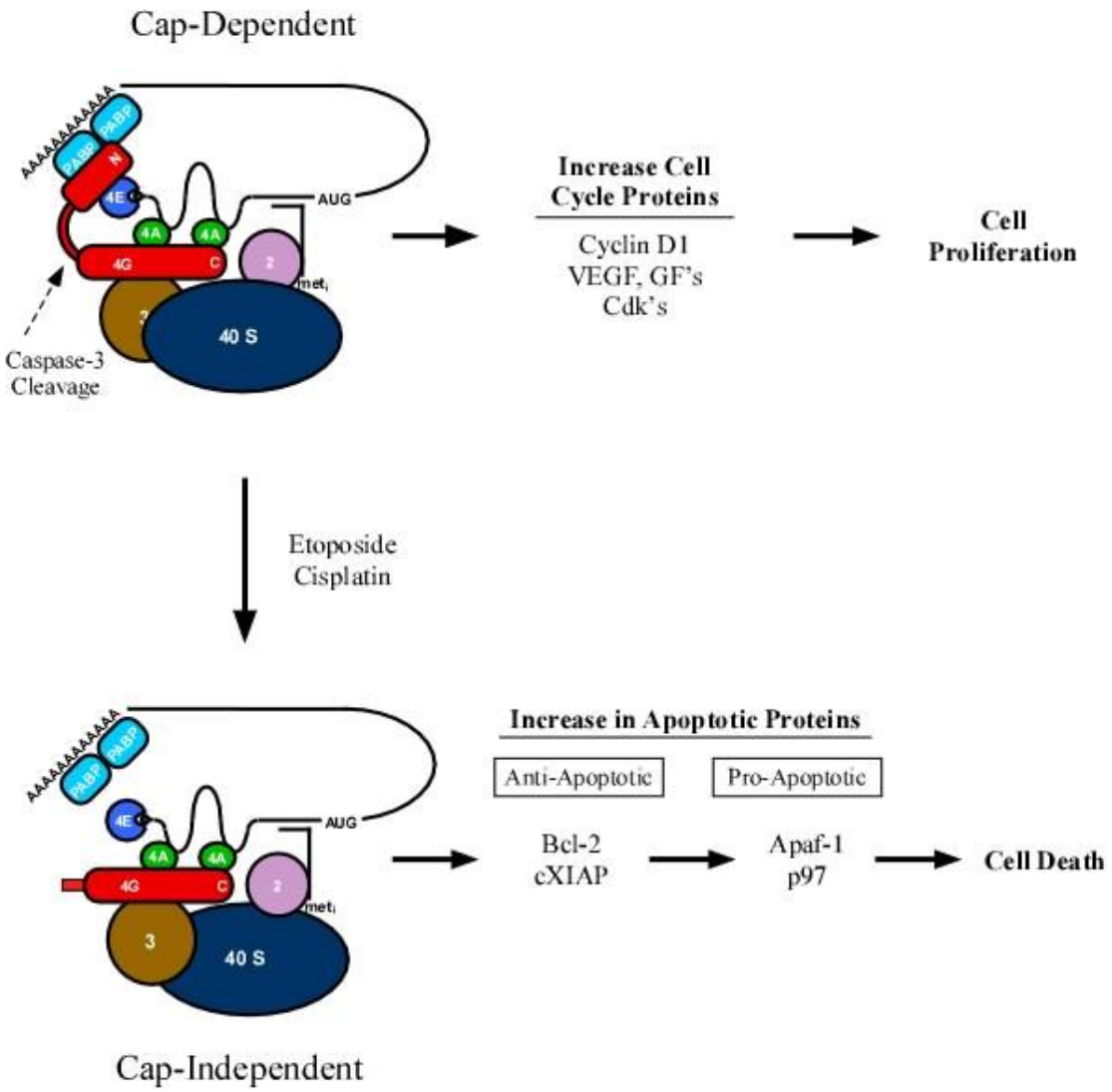

Figure 1. Eukaryotic Initiation Complex: Cap-Dependent vs Cap-Independent Translation Initiation. Cap-dependent translation relies on eIF4G1 to bring together all factors including eIF4E, the 40S subunit and PABP. This mode of translation initiation is known for increasing synthesis of cell cycle proteins and therefore promoting cell proliferation (De Benedetti and Graff 2004; Byrd, Zamora et al. 2005) Upon induction of apoptosis and cleavage of eIF4G at the N-terminal the mechanism of initiation may switch to cap-independent translation. Much of the known cap-independent initiation relies on internal ribosome entry sites (IRES) and occurs without PABP and eIF4E. (Keiper, Gan et al. 1999)

Internal Ribosome Entry Site (IRES)

IRESs were first discovered in positive strand RNA in viruses. Picornaviruses in particular displayed a number of traits that suggested the traditional cap-binding and scanning method of initiation might be inhibited. Some viral mRNA's are naturally uncapped with long 5' UTRs, stable secondary structures, and potential upstream initiation codons (Vagner, Galy et al. 2001). These traits prompted the dicistronic test that lead to the formal discovery of IRESs (Komar and Hatzoglou 2005). The IRES was first discovered in the poliovirus and encephylomyocarditis virus (EMCV) by placing their 5' UTR region into an mRNA between two open reading frames (ORF). By doing so, one could see if the downstream ORF was translated independently of the first ORF(Komar and Hatzoglou 2005). The discovery of IRESs in viral mRNA lead to the exploration of cellular mRNA using the same dicistronic assay to find functional IRESs. Upon investigation, IRES elements were found in the 5' UTR's of mRNAs associated with proteins needed in development, differentiation, cell cycle progression, stress, and apoptosis (Komar and Hatzoglou 2005). These IRESs functioned preferentially when there was an inhibition of cap-dependent synthesis.

Inhibition of cap-dependent translation initiation can be attributed to three primary mechanisms: 1) dephosphorylation of 4E- binding protein 1 (4E-BP1) which sequesters eIF4E and prevents the assembly of the eIF4F complex, 2) cleavage of eIF4G in the hinge region, or 3) the cleavage of the poly-A binding proteins (PABP). There are also situations where the levels of cap-dependent translation are naturally low, and therefore IRESs may be more generally utilized for translation initiation. Examples of this can be seen in proteins whose function is restricted to a differentiated cell. Gap junction proteins and certain proteins in dendrites have mRNAs that are translated in an IRES mediated fashion(Vagner, Galy et al. 2001). Overall, 3-5% of cellular

mRNAs use IRES or cap-independent translation initiation when cap-dependent initiation is impaired, and as much as 30% in specialized cells such as vertebrate oocytes (Keiper and Rhoads 1997). This mode of protein synthesis is therefore thought to have a major impact on mechanisms that lead to either cell survival or cell death (Komar and Hatzoglou 2005). Previous studies have shown that cap-dependent translation, or binding of eIF4G-1 to eIF4E, increases translational efficiency of growth factors such as vascular endothelial growth factor (VEGF) and cyclin D1, whereas cap-independent translation stimulates the translation of apoptotic proteins such as Apaf-1 and DAP5 (De Benedetti and Graff 2004; Contreras, Richardson et al. 2008).

Similar to cap-dependent translation initiation factors, there are a number of IRES trans-activating factors (ITAFS) that associate with the IRES to functionally enhance their translation. The mechanism by which ITAFs function is not known, but there are three predominant theories. ITAFS have the ability to travel between the nucleus and the cytoplasm. One theory is dependent upon the level of ITAFS in the cytoplasm; increasing levels of ITAFS in the cytoplasm might correspond to increasing levels of IRES translation. It is also thought that ITAFS may help to recruit the 40S ribosomal subunit directly, or to stabilize the active form of the IRES by initiating conformational changed in the mRNA (Komar and Hatzoglou 2005).

Eukaryotic Initiation Factor 4G-1

eIF4G has been shown to play a critical role in facilitating a particular mode of translation initiation which makes it a logical target for investigating protein synthesis shifts. Cloning of eIF4G has shown the protein is a product of at least three genes. In humans these homologues can be referred to as eIF4G-1, eIF4G-2 (also known as p97 and DAP5) and eIF4G-3 (also known as eIF4GII)(Gradi, Imataka et al. 1998; Bradley, Padovan et al. 2002). eIF4G-1

contains three structural domains: N-terminal domain, core domain, and C-terminal domain. The N-terminal domain of eIF4G binds the cap-binding protein (eIF4E) as well as the poly A binding protein (PABP) which, in turn, bind the 5' mRNA cap and poly-A tail, respectively. The core domain houses the critical sequences necessary for the assembly of the translation complex with eIF3 and ribosomes, while the C-terminal domain plays a regulatory role through the binding of eIF4A and the kinase Mnk1 to aid in initiating the strongest translation(Morino, Imataka et al. 2000; Prevot, Darlix et al. 2003). eIF4G-1 exists in at least eight different mRNA encoding isoform variants, all of which occur strictly in the N-terminal domain (Figure 2). Variations are due the presence of three characterized promoters, numerous alternative splicing opportunities, as well as alternate AUG start codons throughout the mRNA. Investigating the representation of eIF4G-1 isoforms could give insight into a cell's propensity to use IRES mediated translation initiation over the cap-dependent method based on potential binding complex variations by these isoforms.

Figure 2

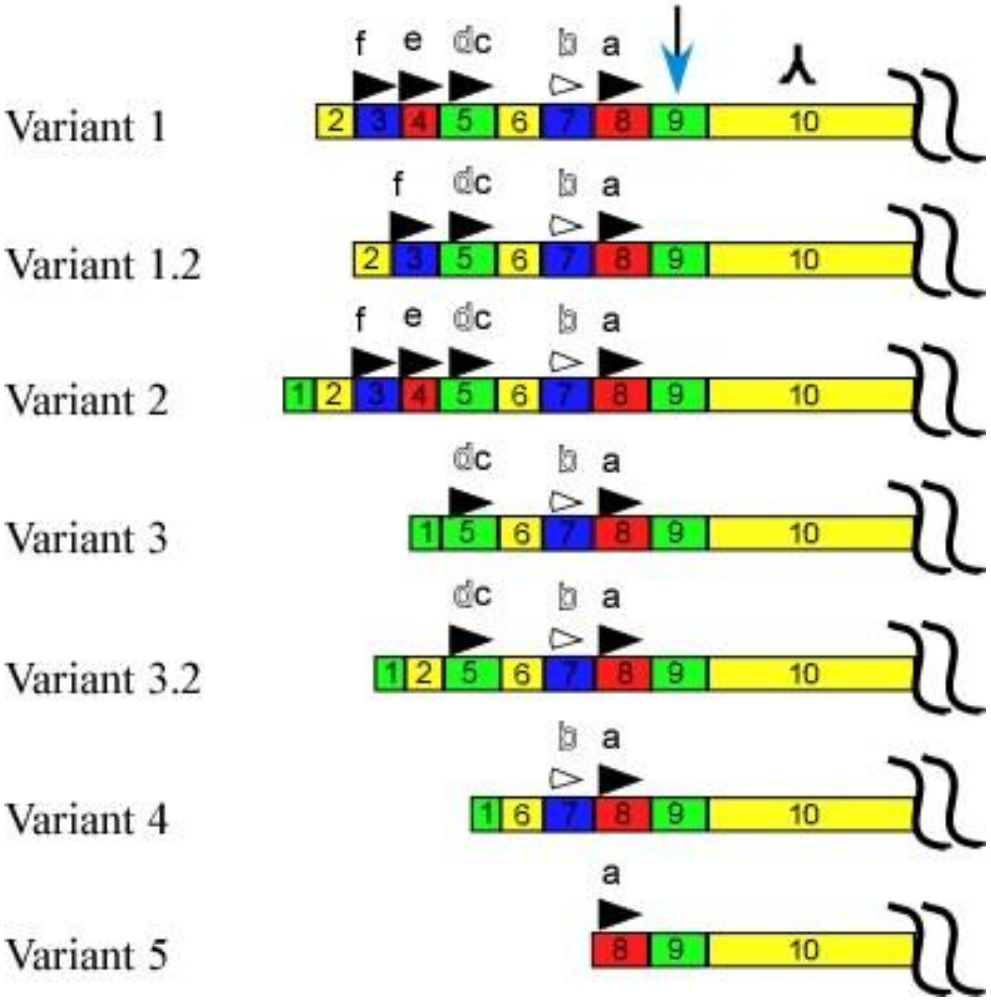

Figure 2. Alternatively spliced eIF4G-1 mRNA isoforms. Isoforms vary in their N-terminal sequences due to multiple promoters, varying initiation start sites and alternative splicing. Black triangles (►) represent varying translation initiation start sites. The symbol (⅄) represents the αZP1 antibody binding site, and (↓) the caspase-3 cleavage site. The first 10 of 33 exons are shown. (Modified from (Coldwell and Morley 2006; Blackwell 2007).

Apoptosis

Apoptosis (programmed cell death) is a natural cellular mechanism required to eliminate extra and damaged cells in order to maintain homeostasis within the organism. A variety of treatments, such as hypoxia, exposure to drugs or toxins, cause the cell to experience a level of stress. Cell stresses and cellular death signals can prompt apoptosis, and induce the release of cytochrome c from the mitochondria. Cytochrome c binds to apoptotic protein Apaf-1 to assemble the apoptosome, which causes activation of caspase-9 and in turn caspase-3. Caspase-3 is considered the executioner of the cell; its activation prompts cleavage of apoptosis regulators, housekeeping proteins, transcription and translation factors, and causes DNA fragmentation, all of which ultimately kill the cell (Nunez, Benedict et al. 1998).

In cases where a functioning caspase is missing apoptosis can also be induced independently of the caspases using Apoptosis-inducing factor (AIF). AIF in humans is transcribed from a gene on the X chromosome, translated in the cytoplasm as a precursor protein, and then transported to the inner mitochondrial membrane where the mature AIF binds and remains until it receives cell stress signals (Modjtahedi, Giordanetto et al. 2006). Hypoxia, DNA damage and activation of poly(ADP-ribose)polymerase (PARP) can all act as signals for the release of AIF from the inner mitochondrial membrane. When one or more of these factors permeate the outer mitochondrial membrane AIF is cleaved and released into the cytoplasm. Once released from the mitochondria cytoplasmic AIF can inhibit protein synthesis by inhibiting the translation of eIF3G, or it may migrate to the nucleus to mediate chromatin condensation and DNA fragmentation, ultimately leading to cell death (Joza, Pospisilik et al. 2009).

In cells that undergo an oncogenic transformation (cancer) the apoptotic pathway is often disrupted via mutations in one or more proteins in the apoptotic pathway. Common examples are the overexpression of Bcl-2 and the inactivation of Bax. Bcl-2 blocks the cells ability to undergo programmed cell death, while Bax under normal conditions acts as an apoptotic promoter (Lowe and Lin 2000). In some breast cancer cell lines (e.g. MCF7) the gene encoding the executioner caspase-3 has been disrupted, also crippling the apoptotic response. A cell's ability to maintain the balance between proliferation and cell death is characteristic of a non-cancerous cell. When any part of the balance is disrupted it can lead to an oncogenic state.

Cell stresses and the onset of apoptosis cause a significant decrease in overall translation of cellular mRNA, but at the same time increases translation of selective mRNAs needed to survive the stressors, or to enter apoptosis (Holcik and Sonenberg 2005) (Figure 3). To accomplish these sequential switches, cells begin to use more IRES mediated or cap-independent translation, which does not require binding of the mRNA cap. One of the most common examples of this can be seen in the proteins X-chromosome-linked inhibitor of apoptosis (XIAP) and apoptotic protease activating factor-1 (Apaf-1). Synthesis of both of these proteins is IRES mediated, but XIAP inhibits caspase cleavage to prevent apoptosis under cell stress, while Apaf-1 promotes caspase cleavage and cell death. Apoptotic trigger and the decrease in cap-dependent protein synthesis don't commit a cell to a particular fate; it first sends the cell into a pre-commitment period where it can attempt to recover from the stress (REFERENCE). Once in the pre-commitment period translation of XIAP is increased, halting the caspase cascade, and allowing recovery time. If cell damage is too great then translation of pro-apoptotic proteins, like Apaf-1, will increase and ultimately lead to cell death.

Once cells are committed to cell death, a constant level of Apaf-1 is needed to continue apoptosis. Cleavage of eIF4G-1, carried out by caspase-3, acts as a positive regulator for the translation of Apaf-1 (Marissen, Gradi et al. 2000), and occurs as cells progress deeper into the apoptotic program. Thus, there appears to be sequential utilization of IRESes during apoptosis, first in an attempt to rescue the cell fate, then to push it to the point of no return from cell death. Cleavage of eIF4G-1 forces the cell to switch from cap-dependent translation to cap-independent translation. Cleaved eIF4G-1 for IRES-mediated translation acts as a positive feedback regulator by increasing translation of Apaf-1, which in turn continues the caspase cascade. The use of IRES-mediated translation initiation is not uncommon, and maintaining the shift between cap-dependent and cap-independent translation initiation is important for non-cancerous cells.

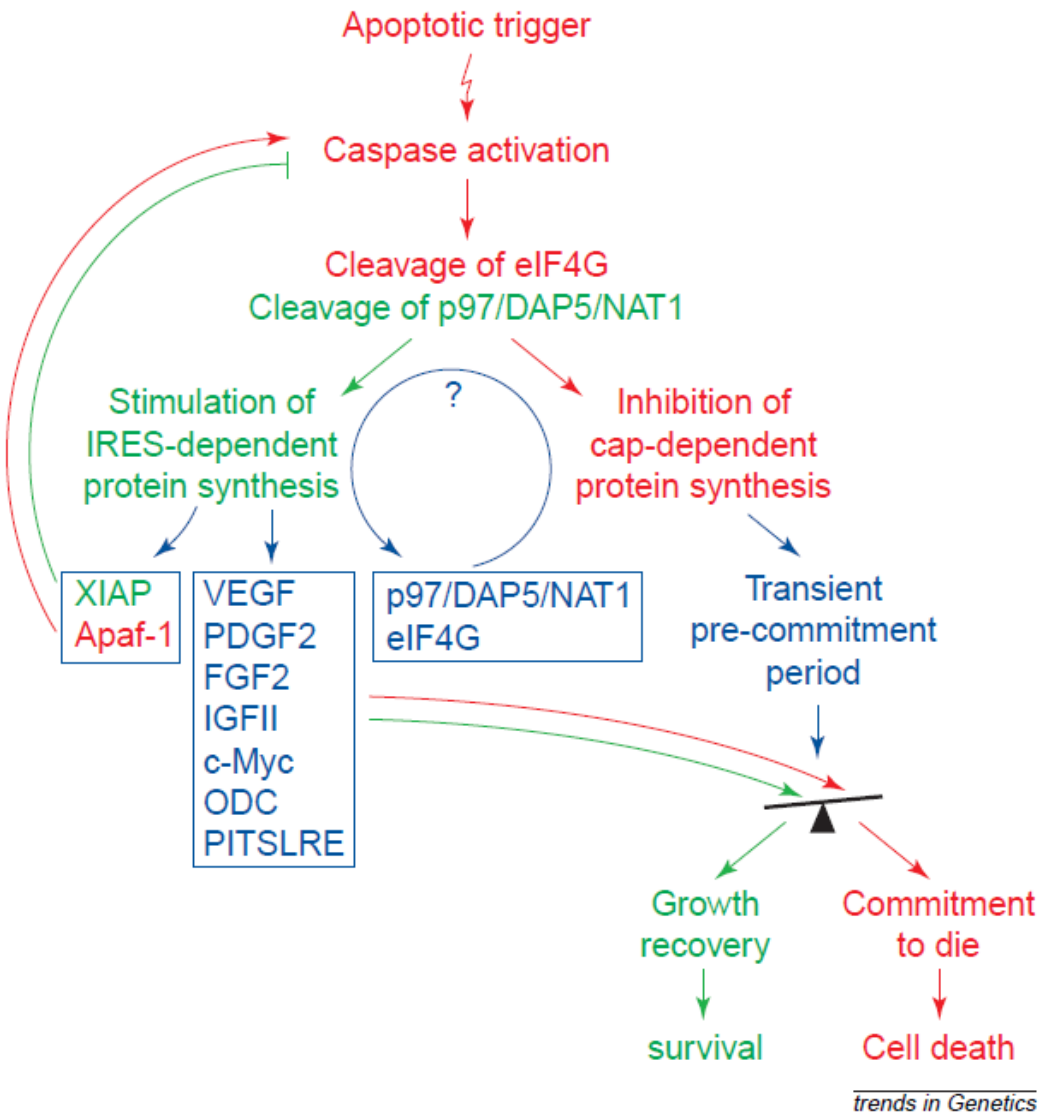

Figure 3. Shifts in protein synthesis occur during apoptosis. Apoptotic triggers cause an overall decrease in cap-dependent protein synthesis while also increasing translation of specific proteins using an IRES-mediated mechanism. This causes first an increase in proteins for cell recovery, and then, if needed, proteins to complete cell death. (Holcik & Sonenburg, 2000)

Chemotherapy Agents

Treatment of breast cancer is typically addressed using a combination of localized treatments, such as radiation therapy, and systemic treatments like chemotherapy. Even though chemotherapy is often used as an adjuvant therapy to surgery, it is still traditionally administered in high doses in the hopes of disrupting cell cycle and proliferation and therefore tumorigenesis (Shapiro and Recht 2001; Drevs, Fakler et al. 2004). Often, chemotherapy drugs are used together, such as Etoposide and Cisplatin, to elicit a maximum response.

The chemotherapy drug, Etoposide, induces single and double DNA strand breaks through inhibition of the enzyme DNA topoisomerase II which aids in DNA unwinding for replication. Inhibition and therefore irreversible DNA strand breaks leads to cell cycle arrest in late S phase or G2 phase preventing cells from completing mitosis. Etoposide is used to treat a variety of tumors such as breast, testicular, small cell lung cancer, and lymphoma (van Maanen, RetÃ¨l et al. 1988).

Cisplatin is a platinum based chemotherapy drug whose mechanism involves binding cellular DNA to form a variety of DNA crosslinks and induce nuclear lesions. Cisplatin induced DNA damage initiates a number of signal transduction pathways, such as MAPK and p53 that ultimately lead to the induction of apoptosis. Cisplatin has a reputation to be one of the most potent chemotherapy agents, but tumor resistance reduces its effectiveness. Some tumors, such as colon cancer, are naturally resistant while others, like ovarian cancer, become resistant over time through decreased drug accumulation and an increase in cell tolerance for DNA damage (Siddik 2003; Alderden, Hall et al. 2006).

The potency of each of these drugs combined with high dosage have negative effects on healthy tissue and can cause a number of side effects including nausea and vomiting, decreased white blood cell count, fatigue and ovarian failure (Cox, Burton et al. 1989; Shapiro and Recht 2001). Chemotherapeutic drugs work to induce apoptosis in cells over a relatively non-specific area. If cancerous cells could be targeted more specifically by manipulating protein synthesis mechanisms and enhancing cap-independent translation a bias for cell death could be created. Chemotherapy drugs at lower dosages combined with cells manipulated to have an affinity for cell death could improve the effectiveness of the treatment, and overall health of surrounding non-cancerous tissues.

MCF10A, MCF7, T47D, and MDA-MB231 Cell Lines

MCF10A, MCF7, T47D, and MDA-MB231 human breast cell lines were cultured for all objectives of the project (Table 1) (ATCC, 2008)**.** MCF10As are an immortalized breast non-tumorogenic epithelial cell line, and were used as a control. MCF7 and T47D are both from patient pleural effusions, estrogen receptor-positive and similar in their aggressiveness. These two cell lines differ in their apoptotic pathways, however. MCF7 cells do not have a functional caspase-3 gene and use primarily a caspase-independent apoptotic pathway; therefore cleavage of eIF4G-1 will be delayed (Janicke, Sprengart et al. 1998). T47D cells have a fully functional caspase-3 gene and are expected to change translation efficiency more readily upon apoptosis. MDA-MB231 is a metastatic, estrogen receptor-negative cell line which forms tumors in not only nude mice, but in BALB/c mice. For this reason it is considered the most aggressive of breast cancer cell lines. None of these cell lines overexpress HER2/neu receptors, but the MDA-MB231 cells do have high levels of the epidermal growth factor receptor type 1 (EGFR-1),

which also contributes to the more aggressive growth and invasion of this cell line (Konecny, Pegram et al. 2006).

Table 1. Characteristics of the human breast epithelial cell line MCF10A, and the breast cancer cell lines MCF7, T47D, and MDA-MB231.

Cell Line	1º or Metastatic	Type	Tumorogenic in nude mice	ER dependent	HER2/neu overexpression
MCF10A	n/a	Non-tumogenic	no	n/a	no
MCF7	metastatic	adenocarcinoma	yes	yes	no
T47D	metastatic	Infiltrating ductal carcinoma	yes	yes	no
MDA-MB231	metastatic	adenocarcinoma	yes	no	no

Objectives:

Objective 1: eIF4G-1 Isoform Representation

Introduction

Of all newly diagnosed cancer cases, breast cancer continues to rank number one among women (Jemal, Siegel et al. 2010). Many factors play a role in keeping the balance between healthy and cancerous cells, one of which is the cell's ability to know when and how to enter programmed cell death (apoptosis) if proliferation becomes irregular. One way to preserve the balance is regulation of protein synthesis mechanism, which consumes close to 90% of the cell's energy under growth conditions. Protein synthesis is generally regulated at the level of initiation on cellular mRNAs. Specifically, natural initiation mechanisms that are mRNA cap-dependent and cap-independent are both at work within the cell (reviewd in (Keiper, Gan et al. 1999)). The ability for the eIF4 initiation complex to form and associate with mRNA is the rate limiting step. Cap-dependent initiation requires that intact, full length eIF4G, a protein critical to create the pre-initiation complex, is able to bind the 7-methylguanosine mRNA cap binding protein eIF4E. Proteins associated with growth and proliferation are nearly all synthesized using this mechanism (Keiper, Gan et al. 1999; Byrd, Zamora et al. 2002; De Benedetti and Graff 2004). Conversely, initiation can occur cap-independently on some cellular (and viral) mRNAs through Internal Ribosome Entry Sites (IRES) which encode internal AUG start sites to begin protein synthesis which eliminate the need for eIF4E and its association with eIF4G to recruit mRNAs via the cap.

While cap-dependent translation initiation predominates in the rapidly growing eukaryotic cells used in most ex vivo studies, quiescent cells appear to conduct as much as 70% of their protein synthesis initiation by a cap-independent mechanism (Keiper and Rhoads 1997).

These observations suggest that a balance of protein synthesis mechanisms may be used to gauge the cell's physiological state. Consistent with this hypothesis, cap-independent initiation has been seen to increase after cell stress or the start of apoptosis (Holcik and Sonenberg 2005; Komar and Hatzoglou 2005). In this case caspase-3 activation brings about a significant decrease in overall translation of cellular mRNA's that require cap-binding, while at the same time increasing translation of selective mRNAs needed to survive the stressors, or eventually to enter apoptosis (Holcik and Sonenberg 2005). To accomplish these sequential switches, cells begin to use more IRES mediated or cap-independent translation, which does not require binding of the mRNA cap.

While relatively few cellular proteins are translated via IRES-driven initiation, key proteins associated with apoptosis, like Apaf-1, Bcl-2, cXIAP and p97, use IRESs to initiate synthesis (Keiper, Gan et al. 1999; Contreras, Richardson et al. 2008). The onset of apoptosis causes a significant decrease in overall translation of cellular mRNA, but at the same time increases translation of a selective subset of mRNAs, via IRESes, needed to either survive the stressors, or to enter apoptosis (Holcik and Sonenberg 2005). IRES dependent translation can play a crucial role in cell survival during temporary stressors. Such is the case with cXIAP, an apoptosis inhibitor, which is found in higher concentration after acute extrinsic stress. IRES driven anti-apoptotic proteins enable cells a rapid mechanism to delay the onset of apoptosis when overall protein synthesis is slowing (Holcik, Sonenberg et al. 2000; Holcik and Sonenberg 2005). If conditions never become favorable for cell survival, or cell damage is too severe those IRES mediated proteins promoting apoptosis, like Apaf-1 and p97, are upregulated. Upon caspase-3 activation and eIF4G-1 cleavage the Apaf-1 IRES is induced, and Apaf-1 protein synthesis increases. After the initiation of apoptosis a constant level of Apaf-1 is needed to carry

out cell death. Cleaved eIF4G-1 itself, along with its homolog p97, act as positive feedback regulators for the Apaf-1 IRES by using their own IRESes to encourage translation in a cap-independent manner, and push a cell into apoptosis (Marissen and Lloyd 1998; Holcik and Sonenberg 2005). This mechanism of an inducible IRES contrasts with many viral IRES activity. Viral IRESes, like the encephalomyocarditis virus (EMCV), have constitutive activity allowing it to be used as a positive control (Jang, KrÃ¤usslich et al. 1988).

eIF4G plays the deciding role between these two forms of initiation, and exists in at least five isoforms that vary in their N-terminal lengths. The nature and physiological significance of this variation in the region bound by eIF4E and the poly(A) binding protein (PABP) is not well understood. We hypothesize that the variations in isoforms and their representation in various cell types play a role in determining cap-dependent versus cap-independent translation initiation. Furthermore, structural alteration of eIF4G isoforms to caspase-3-cleaved forms that promote apoptosis will be highly represented during induction of cell death.

eIF4G-1 isoform representation was determined through western blotting of cell lysates from each of the four breast cell lines. We expected to see a different isoform profile between each cell line due to their oncogenic properties, particularly between MCF10A and MDA-MB231. MCF10A's, being non-tumorogenic, should have a more regulated induction of cell death and are expected to use more readily a different set of isoforms than the MDA-MB231s. The MDA-MB231 cells, representing our most aggressive cell line, are estrogen receptor independent and have high levels of proliferation, so it is expected they will have a higher representation of isoforms that support proliferation. The various isoform representations may contribute to different levels of cap-dependent versus cap-independent translation initiation within each cell line.

In addition to eIF4G isoform representation we wanted to investigate the integrity of poly (ADP-ribose) polymerase (PARP) and p97 (NAT1;DAP5) present in each cell line. PARP is a constitutively expressed nuclear protein whose main function is DNA break repair. Its cleavage by caspase-3 is an early hallmark indicator of early progression in apoptosis. PARP (113kDa) is comprised of 3 domains including a N-Terminal domain which functions for DNA binding, a C-Terminal domain with catalytic activity, and a central domain which functions for auto modifications. Upon DNA damage PARP binds at the damage site and used NAD+ to synthesize poly (ADP-ribose) which ultimately opens the damaged DNA and allow access to DNA repair proteins (Duriez and Shah 1997). PARP is one of the earliest targets of caspase-3 during apoptosis, and is cleaved in the N-terminal to form 89kDa and 24kDa fragments. The signature 89kDa fragment of PARP can be easily detected shortly after induction of apoptosis, therefore cleavage of PARP can, and will, act as an indicator of apoptosis (Duriez and Shah 1997). p97 is a functional isoform of eIF4G lacking the N-terminal region which includes the eIF4E (cap-binding protein) site, and uses an IRES to mediate translation initiation independent of the 5' mRNA cap. p97 has 28% identity to the C-terminal portion of eIF4G1 resembles the shortest isoform of eIF4G-1. It has also been shown to interact with 4A and eIF3 but does not contain a binding site for eIF4E (Imataka, Olsen et al. 1997; Morley, Coldwell et al. 2005). Upon apoptosis, p97 (97kDa) is cleaved at the C-terminal end to form p86 (86kDa) (Henis-Korenblit, Strumpf et al. 2000). Investigating the levels and extent of cleavage of p97 within each cell line can give an indication of caspase-3 activation and the amount of cap-independent translation occurring under given growth or cell death conditions.

Materials and Methods

I. Reagents

Dulbecco's modified Eagle's medium/Ham's F-12 nutrient mixture (DMEM/F12) (+ L-glutamine, -HEPES, High glucose), heat inactivated equine serum (HS), Roswell Park Memorial Institute (RPMI) 1640 medium (+ 4.5g/L D-glucose, +110mg/L Sodium Pyruvate, -L-Glutamine) Dulbecco's modified Eagle's medium (DMEM) (+L-glutamine, 25mM HEPES), heat inactivated fetal bovine serum (FBS), epidermal growth factor (EGF), insulin, gentamicin and OptiMem medium were all obtained from Invitrogen Inc. Cholera Toxin was obtained from BIOMOL. Hydrocortisone, etoposide, and cisplatin were obtained from Sigma. Unless otherwise noted, all other reagents were obtained from Fischer Scientific, Inc.

II. Cell Culture

MCF10A (ATCC: CRL-10317), MCF7 (ATCC: HTB-22) and MDA-MB231 cells (ATCC: HTB-26) cells were obtained from ATCC in Manassas, VA. T47D cells (ATCC: HTB-133) were a gift from Dr. Kathryn Verbanac, Brody School of Medicine, East Carolina University. All cells were grown at 37°C with an atmosphere of 5% CO_2. MCF10A were cultured in DMEM/F12 medium with 10% HS, 10µg/mL insulin, 10 µg/mL gentamicin, 20 ng/mL EGF, 100 ng/mL cholera toxin and 535 ng/mL hydrocortisone (DMEM/F12 complete). MCF7s and T47Ds were cultured in RPMI 1640 medium with 10% FBS 10µg/mL insulin,10µg/mL gentamicin (RPMI Complete). MDA-MB231 were cultured in DMEM medium with 10% FBS,10µg/mL gentamicin (DMEM complete). Cells were harvested at ~80-90% confluency unless otherwise noted by rinsing with phosphate buffered saline (PBS) and using 1X Trypsin (2X Trypsin for MCF10A) (0.5% Trypsin-EDTA (Invitrogen)) at 37°C in 5% CO_2 for

approximately 5 minutes. Cells were collected by centrifugation at 2,000g for about 5 minutes and resuspended in complete medium at a ratio of 1:3 for reseeding or in the appropriate solution for various assays.

I. Preparation of Cell Lystates

Cell lysates were prepared using a modified Radio-immunoprecipitation assay (RIPA) buffer protocol as follows (Blackwell 2007): After trypsinization/centrifugation the cells were washed 3 times with one mL of PBS and centrifuged for 30 sec at 14,000 x g at room temperature in a 1.7mL Eppendorf tube. The cell pellets were lysed with 110µL of modified RIPA buffer [(25mM Tris, pH 7.4, 50mM sodium chloride, 5mM EDTA, 1% Trition X100, 1mM phenylmethylsulfonyl fluoride (PMSF)], and one mammalian protease complete inhibitor cocktail tablet (Roche)). The cell pellet was kept on ice and vortexed every 5 minutes for 15 minutes total. The sample was centrifuged again at 14,000 x g for 10 minutes at room temperature. Supernatent (~100µL) was collected and protein analysis was conducted using a Spot Assay (see below) with Bovine Serum Albumin standards. The lysates were stored at -80°C.

II. Protein Spot Assay

Lysate samples were diluted 1:10 and BSA standards ranging from 0µg/µL - 2.5µg/µL diluted 1:3 in 4X SDS loading buffer lacking beta-mercaptoethanol and bromophenol blue. Samples and standards were boiled at 100°C for approximately 5 minutes. 2µL of sample and 3µL of standard were loaded onto a pre-wet polyvinylidene difluoride (PVDF) membrane (Millipore), stained in Coomassie blue stain for about 15 minutes, and destained (45% MeOH,

10% Acetic Acid) ~20min. Samples were visually compared to standards and concentrations estimated based on standards intensity.

III. Western Blotting for eIF4G-1

Discontinuous sodium dodecyl sulfate-polyacrylamide gel electrophoresis (SDS-PAGE) analysis for eIF4G-1 was carried out using the MiniVE (Hoefer) electrophoresis system; analysis of β-Actin used the Mighty Small (Hoefer) electrophoresis system. Electrophoretic transfer of both eIF4G-1 and β-Actin was carried out using Bio-Rad mini-transfer Blot cell system. 20µg of protein was electrophoresed through a 3.75% stacking gel at 80V (50V for β-Actin) constant voltage followed by resolution on a 5% (38:1) resolving gel at 100V constant voltage or 10% (38:1) resolving gel at 60V constant voltage for eIF4G-1 and β-Actin, respectively. Each was transferred to a PVDF membrane at 200mAmp for 2 hours. Membranes were placed in 5% w/v non-fat milk in TST (10mM Tris-HCL pH 7.4, 150mM NaCl, 0.05% (w/v) Tween 20) overnight in 4°C in order to block all non-specific binding sites. The membranes were then washed three times in TST for five minutes and incubated in the primary antibody ZP1 (1:2000 dilution) in 5% non-fat milk in TST for one hour. The ZP1 antibody is a rabbit polycolonal antibody specific to a peptide derived from exon 10 of the N-terminus domain of eIF4G-1. Membranes were washed three more times for 5 minutes each using TST, then placed in the secondary antibody, a goat anti-rabbit conjugated to horse radish peroxidase (HRP) (Vector Labs), for one hour (1:2000 dilution) in 5% non-fat milk in TST. After incubation the membranes were washed in TST for five minutes each using. Visualization of proteins was done using ECL+ detection reagent (Amersham biosciences/GE) on a Typhoon 9400 Imaging system (Amersham Biosciences). Images were quantified using ImgaeQuant TL and data computed and compiled in Microsoft Excel software.

IV. Western Blotting for p97(NAT1;DAP5)

SDS-PAGE analysis of PARP and p97 was conducted using the same electrophoresis system and electrophoretic transfer system as eIF4G-1. 60µg of protein was resolved on a 3.75% stacking gel at 75V constant voltage followed by a 10% (38:1) resolving gel at 100V constant voltage Samples were transferred to a PVDF membrane at 200mAmp for 2 hours and placed in 5% non-fat milk in TST overnight in 4°C for non-specific blocking. The membranes were washed 3 times for 5 minutes in TST, cut in half for probing, and incubated in the primary antibody, a mouse monoclonal anti-PARP (1:1000), anti-NAT1/p97(1:1000) (BD Transduction Labs) or anti-β-Actin (1:2000) (Sigma), respectively, in 5% non-fat milk in TST, for approximately 1 hour. The membranes were washed three times for five minutes in TST, and incubated in the secondary antibody; a rabbit anti-mouse conjugated to HRP or goat anti-rabbit conjugated to HRP (1:2000 dilution), respectively, for 1 hour. After incubation membranes were washed with TST three times for 5 minutes and visualized using the ECL+ detection reagent and Typhoon 9400 Imaging system. Images were analyzed using ImageQuant TL software.

Results:

I. eIF4G-1 Isoform Representation in Divergent Breast Cancer Cell Lines

Investigating the representation of eIF4G-1 isoforms could give insight into when a cell uses IRES mediated translation initiation over the cap-dependent method. To accomplish this immunoblotting using total protein lysates from each of our four breast cancer cell lines was undertaken. Each human breast cell line represents a different level of aggressive growth but are otherwise unrelated. eIF4G-1 isoform variant a, b, c, e, and f were previously identified using MALDI-TOF-MS (Bradley, Padovan et al. 2002), but only five of the eight total variants,

were able to be resolved using unique SDS-PAGE conditions optimized for resolution of these large, aberrantly migrating proteins (Bradley, Padovan et al. 2002). The longest variant was designated f, and the shortest a, consistent with nomenclature introduced previously by Bradley, et al. (Bradley, Padovan et al. 2002)(Figure 4A). Isoform d could not be electrophoretically resolved by these authors due to its similarity in size to isoform c. Our preliminary findings showed some variation in isoform representation between MCF10A and MCF7 cell lines (Blackwell 2007). These findings suggested an elevated level of the longer isoforms f and e in the slow-growing, non-tumorogenic MCF10A cell line, compared with the fast-growing tumorogenic MCF7 cell line, in which all isoforms were, represented relatively evenly (data not shown). We therefore undertook a more systematic characterization of the five detectable isoforms in all four breast cell lines. However, after determining the percent representation for each isoform in multiple replicate lysates, no systematic increase or decrease across cell lines was evident (Figure 4B). In each breast cancer cell line, regardless of 'aggressiveness', the longer isoforms, f and e, were more prominent than the shorter isoforms. Minor trends, such as slightly elevated levels of isoforms e and f from MCF10A to the MDA-MB231 cells, were not statistically relevant. Little, if any, increase in total eIF4G-1 content, as has been suggested from other studies, was noted in our analyses, suggesting that such increases are perhaps by chance and not causal for growth characteristics (Morley, Curtis et al. 1997; Morley, Coldwell et al. 2005).

Figure 4

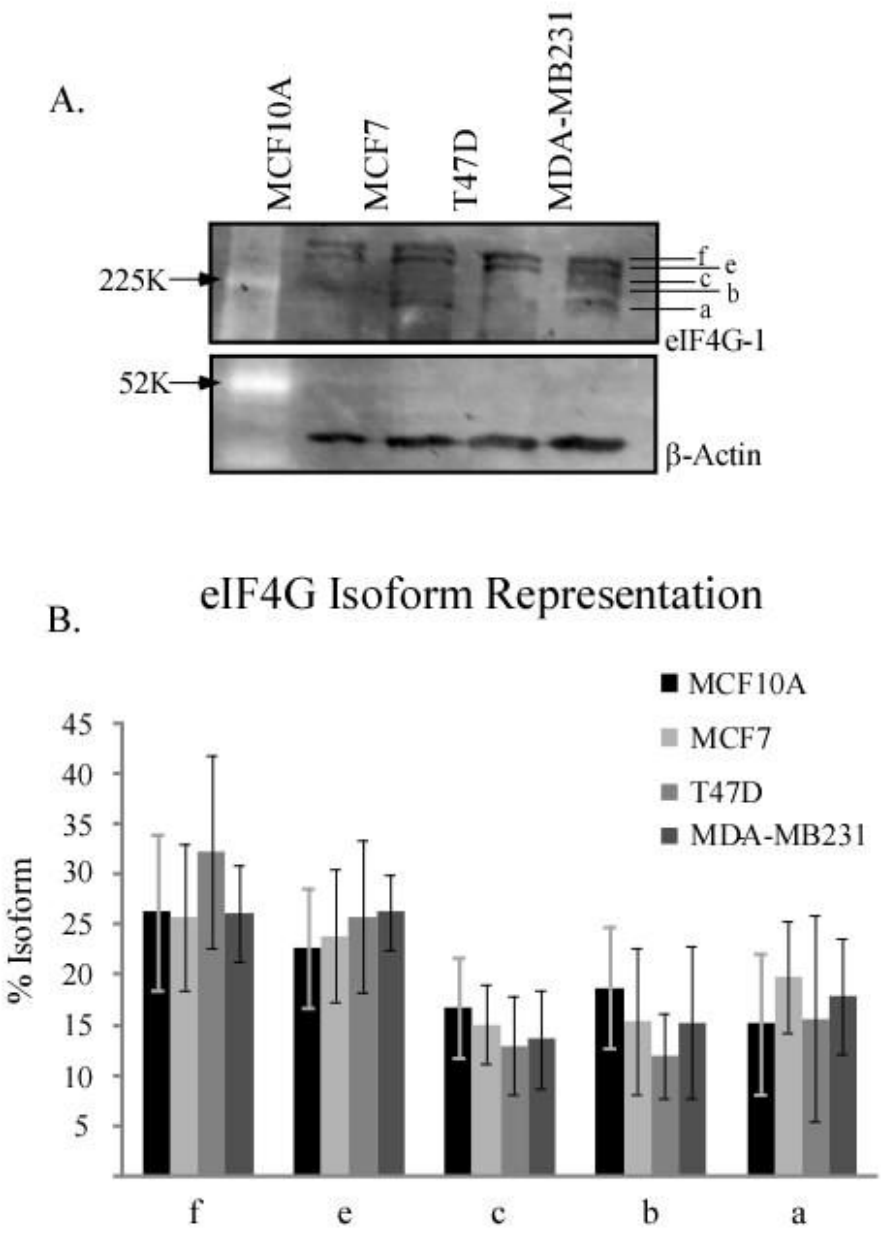

Figure 4. eIF4G-1 Isoform Representation. A. Western blot analysis of eIF4G-1 isoforms run on a 5% (38:1) SDS-PAGE gel. Samples were probed with α-ZPI (eIF4G N-term) pAb (1:2000). Longest isoform variation is labeled as f, shortest as a. (as labeled in (Bradley, Padovan et al. 2002)) Isoforms normalized to actin. B. % Representation of eIF4G-1 isoforms. Standard deviation calculated from N=10 lysates.

II. Variations in eIF4G-p97 Levels in Breast Cancer Lines

The same total protein lysates from each of the breast cancer cell lines was used to determine eIF4G-1 isoform representation by immunoblotting for the eIF4G cap-independent homolog, p97 (NAT1, DAP5). p97 is a functional eIF4G that naturally lacks the N-terminal region to which eIF4E (cap-binding protein) binds. Interestingly, synthesis from p97 mRNA uses an IRES to mediate translation initiation independent of the 5' mRNA cap (Morley, Coldwell et al. 2005). Upon apoptosis, p97 (97kDa) is cleaved by caspase-3 to form p86 (86kDa), a structurally modify version that remains active in cap-independent initiation (Henis-Korenblit, Strumpf et al. 2000). Investigating the levels of p97 within each cell line can give an indication of the amount of cap-independent translation occurring natively in those cells. Western blotting for p97 showed a distinct band at ~97 kDa (Figure 5A) with a less prominent band migrating slightly faster, which is characteristic of p97 upon efficient electrophoretic gel resolution (Henis-Korenblit, Strumpf et al. 2000). When normalized to β-actin, p97 was consistently found to be more than 2.5-fold more abundant in the MCF7 and T47D tumor-forming cell lines than the MCF10A non-tumor-forming cells (Figure 5B). Curiously, the most aggressively growing breast tumor cell line, MDA-MB231, showed no significant elevation of p97. While no absolute correlation between p97 abundance and tumor formation can be drawn from these data, it is clear that the basal cap-independent activity may be substantially elevated in transformed breast cells even as cap-dependent eIF4G-1 levels remain relatively unchanged. This emphasizes the importance of considering the other eIF4G homologs when evaluating, for example, the correlation of cap-independent initiation with eIF4G-1 (and perhaps eIF4G-II) cleavage.

Figure 5

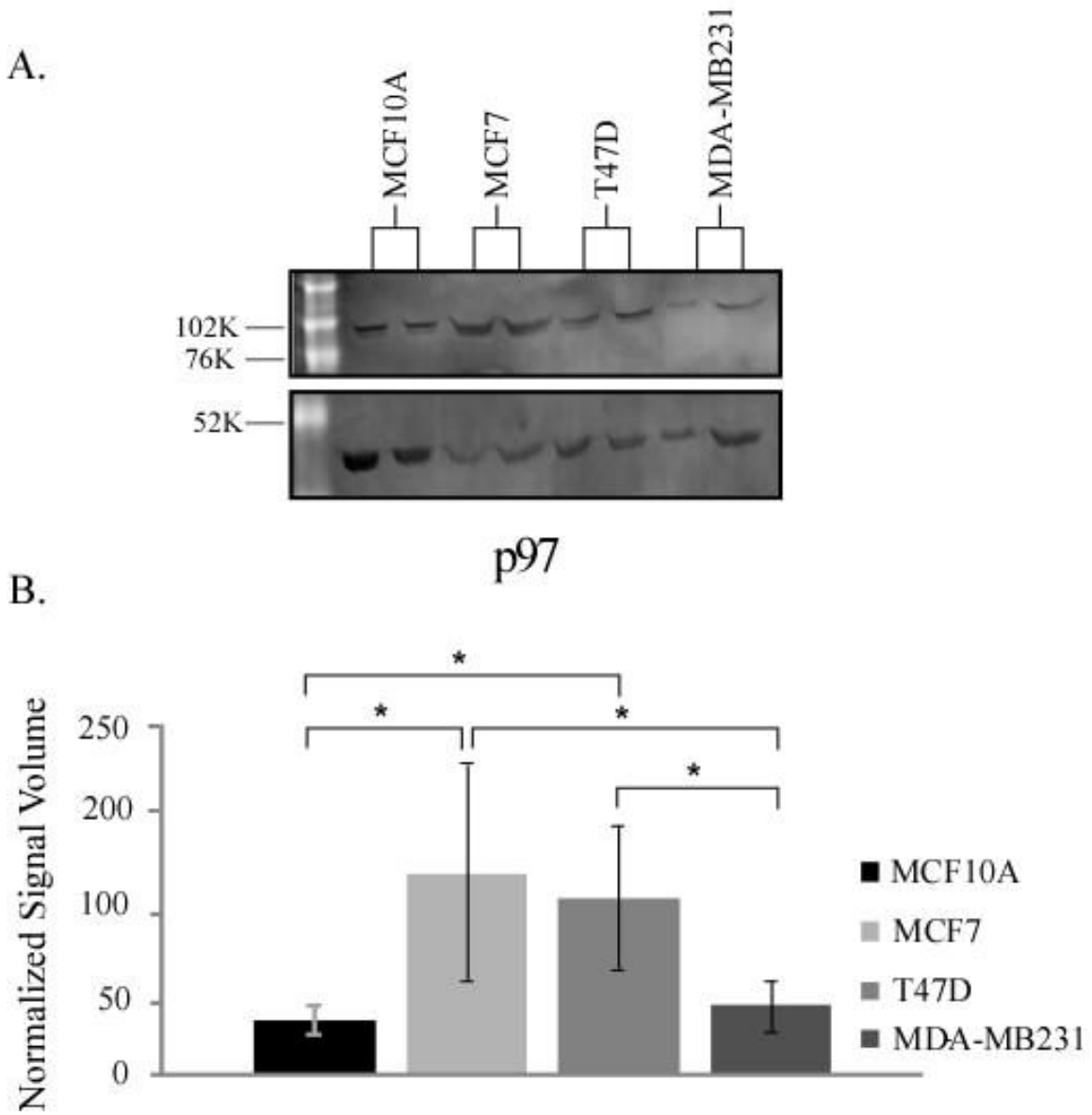

Figure 5. Variations in p97 levels. A. Western blot analysis for p97 run on a 10% (38:1) SDS-PAGE and probed with α-NAT1 (p97) mAb (1:1000). (kDa = 97) Normalized to actin. p97 can appear as a 2 bands depending on gel resolution (Henis-Korenblit, Strumpf et al. 2000) B. Normalized p97 levels. Standard deviation calculated from N=5 samples. * denotes $p < 0.05$.

I. eIF4G-1 Representation and p97 levels in Protein Lysates of Subconfluent Cells

Initial western blotting for eIF4G-1 and p97 were done using cell harvested at ~80% confluency for protein cell lysis. Cells at a higher confluency are not dividing as rapidly, and therefore might not be using the same set of eIF4G isoforms. Due to this, the isoform representation and p97 levels were investigated in cells at lower confluency. Cells were harvested at ~60% confluency, and lysed following the protocol outlined in *Preparation of Cell Lysates*. Immunoblotting with subconfluent lysates for eIF4G isoforms showed slight variation from the initial representation on a smaller scale, but overall did not show any obvious trends between cell lines. The larger isoforms, f and e, were still represented more abundantly as a whole than isoforms c, b, and a. One notable difference between initial and subconfluent westerns is the apparent increasing trend in the smallest isoform, a, across cell lines. MCF10As, the non tumerogenic line, have an abundance of only ~25% compared to the MDA-MB231 cells. While this may be seen in isoform a other isoforms don't show noteworthy patterns. This combined with the higher levels of variation throughout, lead to the conclusion that regardless of confluency at harvesting, no significant trends presented between the four breast cancer cell lines. Western blotting for p97 using subconfluent lysates show almost identical pattern representation across the cell lines. MCF10As and MDA-MB231's once again have lower levels of p97, while MCF7 and T47D have slightly higher levels. Initial (Figure 6B) and subconfluent p97 levels being so close in distribution only further confirms the lack of influence confluencey has on evaluating eIF4G under these circumstances.

Figure 6

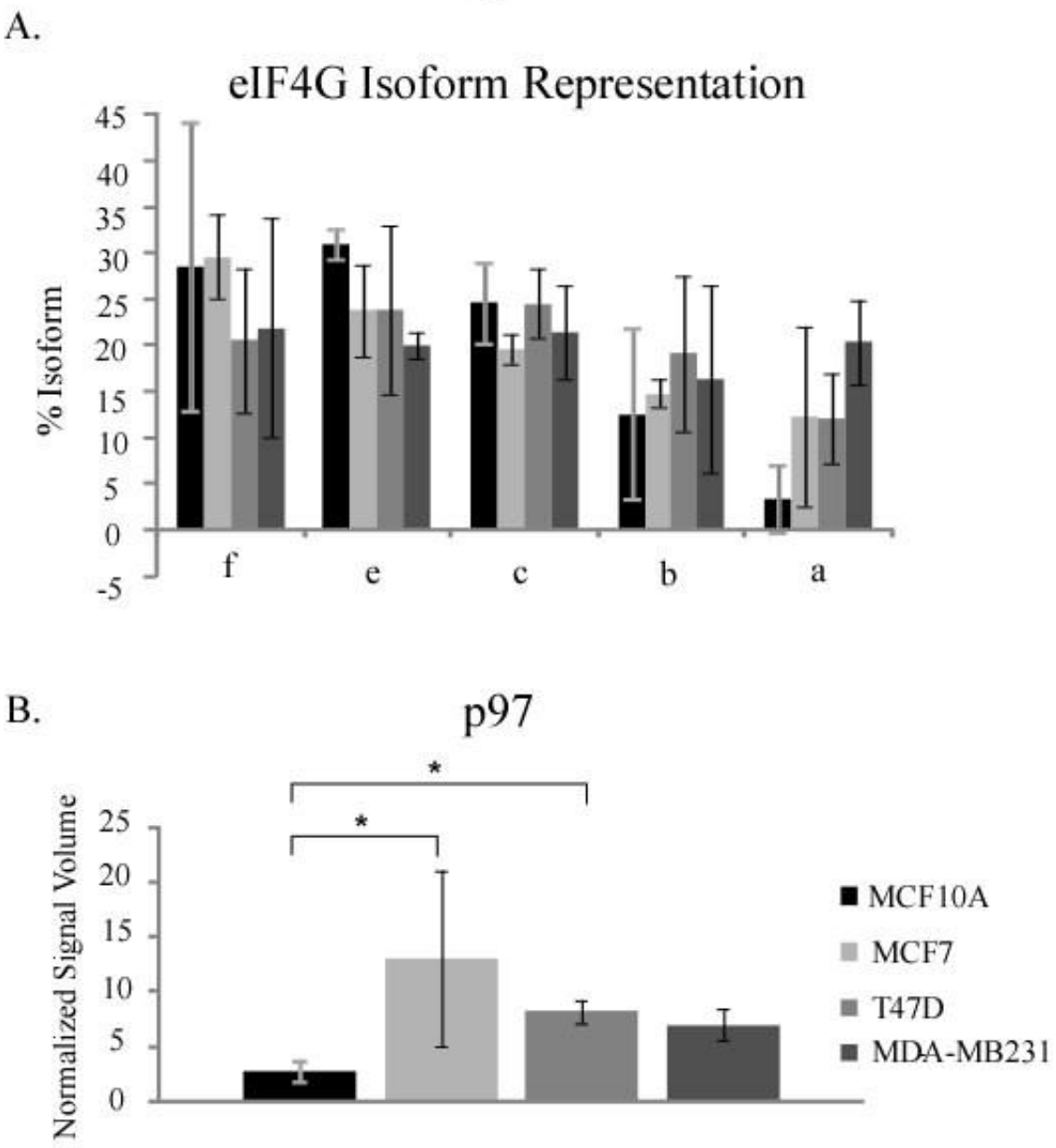

Figure 6: Western Blotting of Subconfluent Protein Lysates. Cells were harvested at ~60% confluency instead of the initial ~80%, and analyzed for eIF4G isoform representation and p97 levels in each cell line. Upon comparison of subconfluent to original lysates it was determined that the level of confluency at harvest does not have a significant effect on either isoform representation or p97 levels in any of the four cell lines. A. eIF4G-1 isoform % representation in subconfluent lysates (N=4). Original % Representation Figure 4B. B. p97 levels in subconfluent lysates (N=4). * denotes $p < 0.05$ Original p97 levels Figure 5B.

Discussion

The importance of multiple isoforms of eIF4G-1 has been questioned since their targeting (p220) by poliovirus protease 2A was clearly observed some 30 years ago (Bonneau and Sonenberg 1987). Bradley, et al were able to definitively characterize structural differences between the isoforms by mass spectrometry as arising from micro-heterogeneity in the N-termini (Bradley, Padovan et al. 2002). The divergence arises from both alternative splicing and alternative translation start site (AUG) selection, and the authors correlated the forms "a" to "f" that may be separated by high-resolution SDS-PAGE with individual, progressively longer N-terminal sequence identities. eIF4G-1 isoforms f and e contain both the eIF4E and PABP binding sites present in exons 7-8 and 10, respectively, both of which are required for cap-dependent translation initiation (Keiper, Gan et al. 1999). The shortest isoform, a, lacks the PABP site but contains most of the eIF4E-binding site. As such it more closely resembles the structure of p97 which facilitates cap-independent initiation, but this activity for eIF4G-1a has not been demonstrated. However, using specific isoform depletion from cultured cells using siRNA, Coldwell and Morley were able to accomplish modest depletion of certain isoforms, and show some variations in translational rates. After targeting exon 4 of eIF4G-1 mRNA, and therefore the longest isoforms, there was an evident depletion of isoform f, a slight decrease in e, and levels of c were maintained. Regardless of the ~50% decrease in overall eIF4G-1 levels, translational rates remained stable, indicating that isoforms e and c were sufficient for restoring cap-dependent translation. Conversely, when exon 3 was targeted for depletion there was a decrease in translational rate and an increase in isoform a, suggesting that the shortest isoform lacks the ability to maintain maximal cap-dependent translation, and is potentially using a

previously characterized eIF4G-1 IRES to mediate translation of its own mRNA (Coldwell and Morley 2006).

If the shorter isoforms, particularly a, rely on IRES mediated translation initiation as suggested under normal, untreated conditions it is possible the lack of abundance of these isoforms is due suppressed apoptotic activity (particularly caspases) occurring in the cells. Rapidly proliferating cells rely heavily on predominantly cap-dependent mechanism (De Benedetti and Graff 2004). Therefore breast cancer cells, particularly those from aggressively growing tumors, would be expected to utilize those isoforms that have all the required binding sites for cap-dependent initiation far more readily. The smaller isoforms that lack all or part of the requirements for cap-dependent translation would be used less frequently until some shift in the predominant mode of translation initiation were to occur (e.g. quiescence). It was therefore not surprising that each breast cell line we analyzed by high resolution SDS-PAGE had a higher abundance of the larger isoforms, f and e, over the smaller forms. What was rather surprising was that this isoform representation was more-or-less constant regardless of the breast cell line cancer stage of the cell line's derivation. The similarity in isoform patterns between cell lines could be due to the fact that all have been adapted from their primary progenitors for ex vivo growth, as well as the lack of apoptosis occurring in these cells.

Objective 2: Determine Predominant Mode of Translation Initiation

Introduction

In order to look into an increase in IRES activity during apoptosis, we undertook to develop a method to determine the predominant mode of translation initiation on a cell to cell basis. In order to do this the ratio of cap-dependent translation to cap-independent translation should be directly measurable in live cells. We proposed to accomplish this through transfection of a dual fluorescence plasmid into breast cancer cells, and comparing levels of blue to green fluorescence. The basic five-component construct of the plasmid consists of the CMV promoter, followed by the gene for blue fluorescence (BFP), next an IRES, the gene for green fluorescence (GFP) with an insulin-like growth factor (IGF2) tag attached, and finally a SV40 polyA addition sequence. Accumulation of blue fluorescence represents cap-dependent translation, and green fluorescence represents cap-independent translation that requires the presence of IRES to initiate ribosomes internally and synthesize GFP. The ratio of blue to green therefore shows a normalized activity for the translation from the IRES in cells under a given physiological condition. By identifying the predominant mode of translation initiation, correlations to the eIF4G-1 isoforms active during initiation could possibly be established. Such a correlation could allow particular eIF4G-1 isoforms associated with proliferation to be knocked down, or those shown to promote apoptosis enhanced, and possibly change a cell's fate.

Figure 7

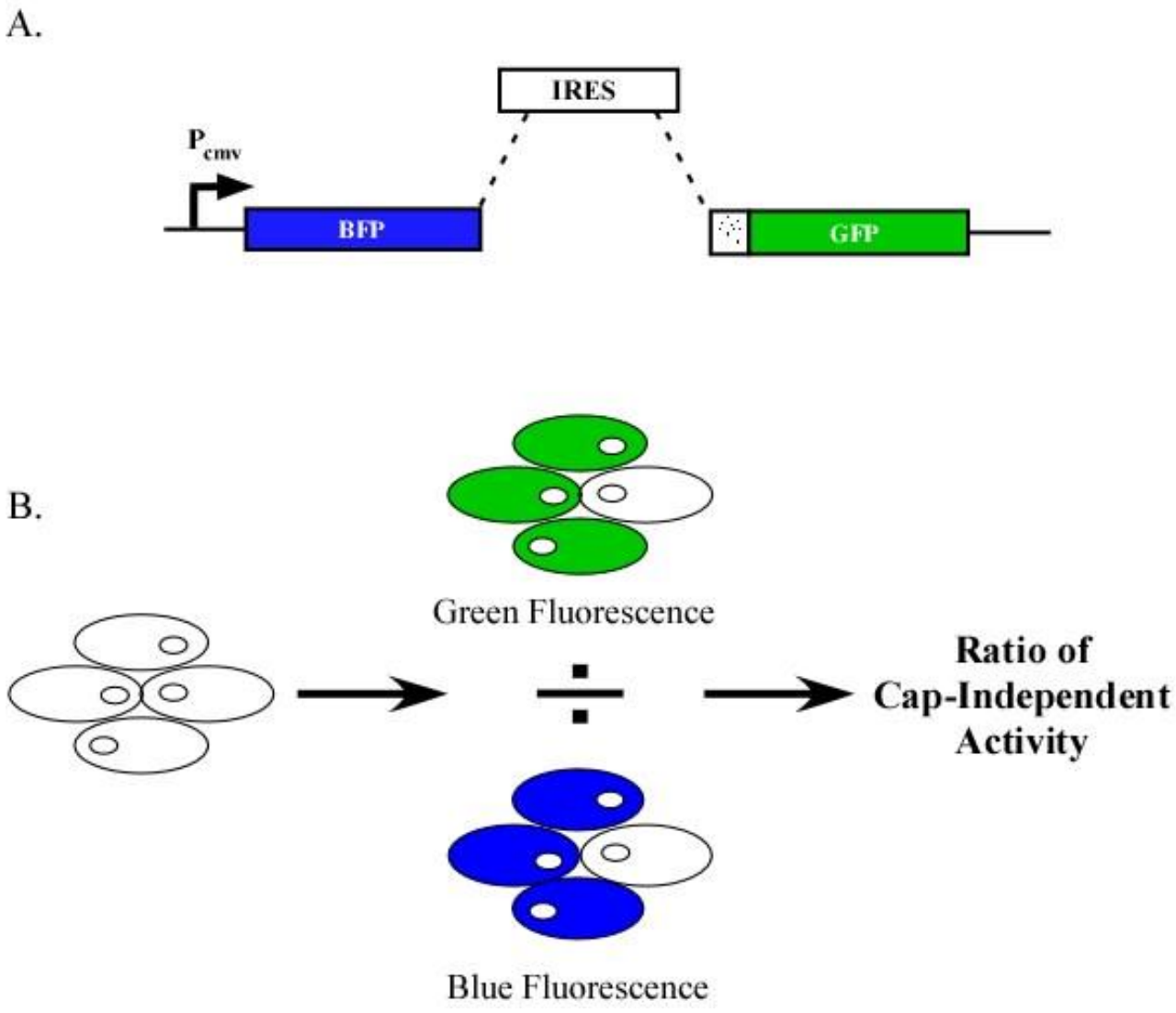

Figure 7. Dual fluorescence reporter plasmid. A: Plasmid schematic. B: Measuring fluorescence output in both blue and green channels after transfection with the dual fluorescence reporter plasmid can act as readout for cap-independent translation initiation occurring in single, live cells.

Four plasmids were used, each encoding a different IRES element (or no IRES). Expression from each plasmid might be expected to promote different blue/green fluorescence ratios. Two reference plasmids expressing either green (GFP) or blue fluorescence (BFP) only were transfected separately (Table 2). The encephalomyocarditis virus IRES (EMCV) is known for initiating high levels of cap-independent translation in mammalian cells under all conditions and was used as a positive control (Bochkov and Palmenberg 2006). Transfections with the EMCV IRES should express both blue and green fluorescence. Blue fluorescence should be consistent throughout all plasmids due to its use of the cap-dependent mode of initiation, whereas the EMCV IRES should promote high levels of cap-independent translation and therefore green fluorescence. The Apaf-1 IRES was used as the experimental IRES, as it is reported to be specifically induced during apoptotic progression. Monitoring Apaf-1 IRES activity allows us to determine the varying levels of cap-dependent and cap-independent initiation taking place within the cell under normal and apoptotic conditions. The Apaf-1 construct should express both blue and green fluorescence, but the degree of each will be based upon the cell's apoptotic activity. When apoptosis is induced we expect to see higher Apaf-1 IRES activity. The Apaf-1 antisense IRES might be expected to act as a negative control, and not yield significant green fluorescence. However, in such complementary sequences there is a possibility that secondary structures associated with the complementary IRES sequence could recruit ribosomes and initiate some translation. The plasmid with no IRES is a true negative control, and should only promote blue fluorescence. To also act as a positive control, two reference plasmids, containing the CMV promoter and either the gene for blue or green fluorescence by itself were used.

Table 2. Expected fluorescence patterns of plasmid constructs (pMax). Different fluorescence patterns are expected depending on the presence or lack of various IRESs. Blue fluorescence indicates cap-dependent initiation while green fluorescence indicates cap-independent initiation.

Plasmid	Blue Fluorescence	Green Fluorescence
EMCV IRES	YES	YES
Apaf-1 IRES	YES	YES
Apaf-1 Antisense IRES	YES	YES/NO
No IRES	YES	NO
BFP Only	YES	NO
GFP Only	NO	YES

Materials and Methods:

I. Subcloning of Expression Plasmids with IRESs

Construction of the bicistronic reporter plasmids pMax-EMCV, pMax-Apaf-1 Sense, pMax-Apaf-1 Antisense, pMax-Apaf-1 Deletion, pMax-BFP, and pMax-iGFP was done using a cloning strategy developed by Dr. Brett Keiper and myself, with technical assistance from Dr. Enhui Hao.

pMax-EMCV (Figure 9) was created using the parent plasmids pCMV-EMCV and pMax-GFP (Figure 8) (gift from Dr. Brian Shewchuk). 10µg of pCMV-EMCV was digested with 5µL of Xba1 overnight at 37 ºC (Table 3). After digestion, the DNA was phenol/chloroform extracted and precipitated with ethanol. After precipitation, a second digest with 5µL of SacI was incubated overnight at 37 ºC, and followed up with a third digest using 5µL of SacII for ~1 hour at 37 ºC. Digestion of pCMV-EMCV produced the BFP-IRES-GFP insert. 10µg pMAX-GFP was digested with 5µL of NheI at 37 ºC overnight, the DNA was phenol/chloroform extracted and ethanol (EtOH) precipitated, and digested a second time with 5µL of SacI at 37 ºC overnight. The digestion of pMax-GFP produced the vector portion of the new construct. Upon completion of all digestions, samples were run on a 1% Agarose gel + 0.5X TBE (Tris, Boric Acid, EDTA) and the appropriate DNA bands for insert (~2.1 kb) and vector (~2.7kb) were cut from the gel. The DNA was extracted from the gel using a Zymoclean DNA Gel Recovery Kit (ZymoResearch) as follows. Both insert and vector were weighed, mixed with 3 volumes of ADB binding buffer in a 1.7mL centrifuge tube and incubated at 55 ºC for 5-10 minutes with periodic vortexing until all the agarose was melted. The melted agarose was added to a Zymo-Spin Column, which was placed into a collection tube, and centrifuged (Eppendorf Centrifuge

5451C) for 1 minute at 12K rpm. Contents in the collection tube was transferred into a clean 1.7mL tube and set aside. 700 µL of Wash Buffer was added to the column, and centrifuged for 1 minute at 14K rpm; this was repeated twice more. The spin column was placed into a new 1.7mL tube, 10µL of nuclease free water was added, and the column was spun at 14K rpm for 1 minute to elute DNA. The elution step was repeated once more, and the tubes were place in the vacuum dry for 2 minutes to remove any remaining EtOH. Both insert and vector were run on a 1% Agarose gel + 0.5X TBE gel to estimate amount of DNA eluted. Ligation reactions were set up at a ratio of 3:1 insert to vector using Takara DNA Ligation Kit and incubated at 15 ºC for one hour. Transformation was completed using 25µL of DH5α E. coli cells which were gently mixed with 1µL of ligated DNA and incubated on ice for 10 minutes. The cells were heat shocked at 42 ºC for 2 minutes, and placed back on ice for an additional 2 minutes. 250µL of S.O.C. Medium (Invitrogen) was added to each tube, and placed on a 37 ºC shaker for ~1 hour. The mixture was plated on a LB + Kanamycin (50µg/mL) plate and placed in a 37 ºC incubator overnight.

Table 3. Restriction Enzyme digestion of pCMV-EMCV and pMax-GFP to create pMax-EMCV.

	pCMV-EMCV (Insert)			pMax-GFP (Vector)	
Digestion #	1	2	3	1	2
DNA	10µg	10µg	10µg	10µg	10µg
Enzyme	Xba1	SacI	SacII	NheI	SacI
Time:	Overnight	Overnight	~1hr	Overnight	Overnight

Upon successful transformation, 10 colonies were harvested for mini-preparation of the plasmid. 10 polystyrene round bottom tubes (BD Falcon) were collected and 2mL of LB + Kanamycin (50µg/mL) was added to each. Using a sterile toothpick a single colony was harvested and placed into the polystyrene tube. The cultures were then placed on a 37 ºC shaker overnight. Samples were removed from the shaker; half the volume of each tube (~1mL) was transferred to a 1.7mL centrifuge tube and spun at 14K x g for 5 minutes. Upon aspiration of the media 100µL of Mini-Prep Solution 1 (25mM Tris pH 8.0, 50mM glucose, 10mM EDTA) was added, tubes were vortexed to resuspend cells, and then incubated for 5 minutes at room temperature. 200µL of Mini-Prep Solution 2 (0.2N NaOH, 1% SDS) was added to each, inverted to mix, and incubated at room temperature for 5 minutes. 150µL of Mini-Prep Solution 3 (5M KAc in glacial acetic acid) was added to each tube, inverted to mix, incubated on ice 5 minutes, and centrifuged at 14K x g for 10 minutes. Supernatant from the spin was transferred to a clean 1.7mL centrifuge tube for phenol/chloroform extraction and ethanol precipitation. After precipitation, the pellet was resuspeneded in 200µL of a water/RNAse A mixture (1µL per 200µL), incubated for 1 hour at 37 ºC, and a portion of each was digested to check plasmid structure.

The plasmid was purified with a large scale cesium chloride (CsCl) preparation as follows. Bacterial cells containing the pMax-EMCV plasmid were grown overnight in 250mL selective medium. Cultures were poured into Beckman 250mL polypropylene GSA Rotator bottles and centrifuged in a Sorvall GSA rotor at 5K x g for 15 minutes at 4 ºC. The cells were resuspended in 5mL of ice cold Mini-Prep Solution 1. 600µL of Lysozyme in stH_2O (12mg/mL) was added to each tube and incubated on ice for 20 minutes. 12mL of Mini-Prep Solution 2 was added to each tube, inverted to mix, and incubated on ice 10 minutes followed by the addition of

7.5mL of Mini-Prep Solution 3 which was mixed by inverting and incubated on ice 10 minutes. The samples were centrifuged at 8K x g (4 ºC) for 25 minutes in a Sorvall GSA rotor. The supernatant was poured through a coffee filter into 50mL polypropylene tubes, then split into 30mL Corex Tubes. An equal volume of 2-Propanol was added to each tube, vortexed, and and incubated 15 minutes at room temperature to precipitate DNA. Samples were spun in an SS34 rotor at 5K x g for 1 hour at 4 ºC. The supernatant was removed and pellet was washed with 70% ethanol. The tubes were covered with parafilm, vented, and dried in a vacuum dryer for 10 minutes. The samples were resuspended in 4mL of TE (10mM Tris pH 8.0, 1mM EDTA with 208µL RNAse A (1mg/mL)) and 0.42mL ethidium bromide (EtBr), then 4.5g CsCl was added to each tube and mixed well until dissolved. Samples were spun at 8K x g in an SS34 rotor for 10 minutes. Supernatant was transferred to Beckman sealable (Ti70) centrifuge tubes and the tubes were weighed and balanced to 0.01g. Tubes were centrifuged overnight using an Optima Max-XP Ultracentrifuge (Beckman Coulter) at 70K x g overnight (20-24hours) at room temperature. The tubes were mounted on a ring stand, and the DNA bands visualized with a UV lamp. The top of the tube was punctured with a 20 gauge syringe which was left in place to allow for air flow. The side of the tube directly below the plasmid DNA band was punctured with a 20 gague needle attached to a 10mL syringe, and was used to extract the band. Samples were transferred into a 15mL polypropylene tube and were extracted 4X each with H_2O saturated with butanol to remove leftover EtBr. Samples were diluted with 9X the volume of TE, and then with 2X the volume of 100% EtOH, then transferred to a 30mL glass tube with labeled sleeve. The tubes were centrifuged in an SS34 rotor at 13K x g for 60 minutes, and the supernatant pourd into 50mL polypropylene tubes. The glass tubes containing the pelleted DNA was rinsed with 5mL of 70% EtOH , dried under vacuum for 10min, and then resuspended in 400µL of sterile H_2O.

Samples were diluted 1:50 and the concentrations were determined using a Shimadzu Pharmaspec UV-1700 spectrophotometer. Plasmid DNA was precipitated with 1/10 the volume of 3M sodium acetate and 2.5 volumes of 100% EtOH which was added to the samples, vortexed, and incubated in -80 ºC for one hour. The samples were centrifuged at 14K x g at 4 ºC for 30 minutes, the pellets rinsed with 70% EtOH, and resuspended in the appropriate volume of sterile H_2O to a final concentration of approximately 1µg/µL. Samples were stored at -20 ºC and the sequences mapped with the program Vector NTI.

pMax-Apaf-1 Sense, pMax-Apaf-1 Antisense, and pMax-Apaf-1 Deletion (Figure 9) were created using the parent plasmids pMax-EMCV (vector) and the corresponding pCMV-IRES construct (insert). 10µg of pMax-EMCV per reaction was digested with 5µL of NheI overnight at 37 ºC, phenol/chloroform extracted, precipitated with EtOH, and digested a second time with BamHI overnight at 37 ºC to create the vector. Each pCMV-IRES plasmid followed the same digestion plan as pMax-EMCV to create the insert portion for each plasmid. Each sample was run on a 1% Agarose + 0.5X TBE gel and the appropriate DNA bands were removed. DNA gel extraction, ligation, transformation, DNA mini-prep, and CsCl purification for each plasmid followed the protocol outlined for the creation of pMax-EMCV.

pMax-BFP and pMax-iGFP (Figure 10) were created using only pMax-EMCV as the parent plasmid. pMax-BFP was constructed by digesting 10µg of pMax-EMCV with 5µL of SmaI for 3 hours at 37 ºC. At the same time, and additional 10µg of pMax-EMCV was digested with 5µL of KpnI under the same conditions to make pMax-iGFP. An additional digest was required for pMax-iGFP; after phenol/chloroform extraction and EtOH precipitation 5µL HindIII was added for 3 hours at 37 ºC. Both samples were run on a 1% Agarose gel + 0.5% TBE and the appropriate bands removed. DNA gel extraction, ligation, transformation, DNA

mini-prep, and CsCl purification for each plasmid followed the protocol outlined for the creation of pMax-EMCV.

Figure 8

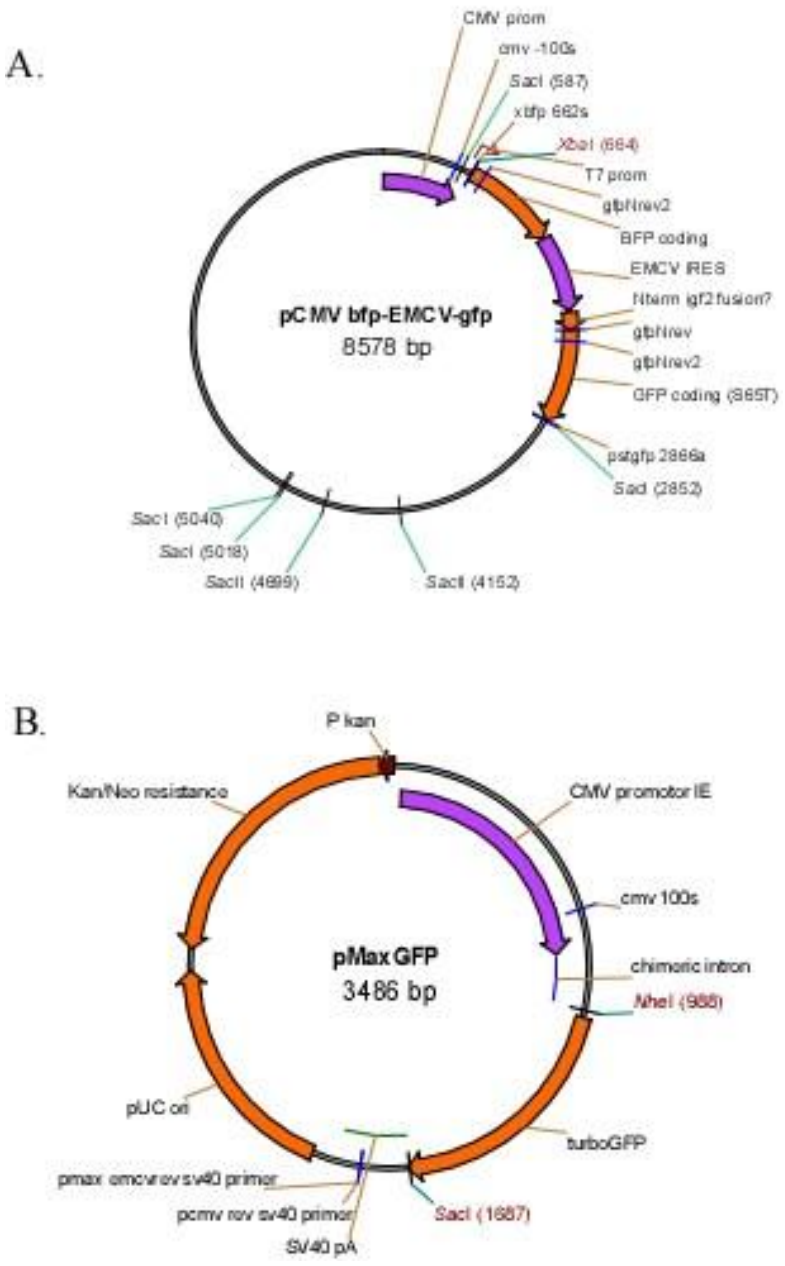

Figure 8. Parent Plasmids used for constructing the pMax- plasmids. The BFP-IRES-GFP portion of the pCMV plasmid was subcloned into pMax-GFP. pMax-GFP was chosen as the vector due to its smaller size and stronger promoter.

Figure 9

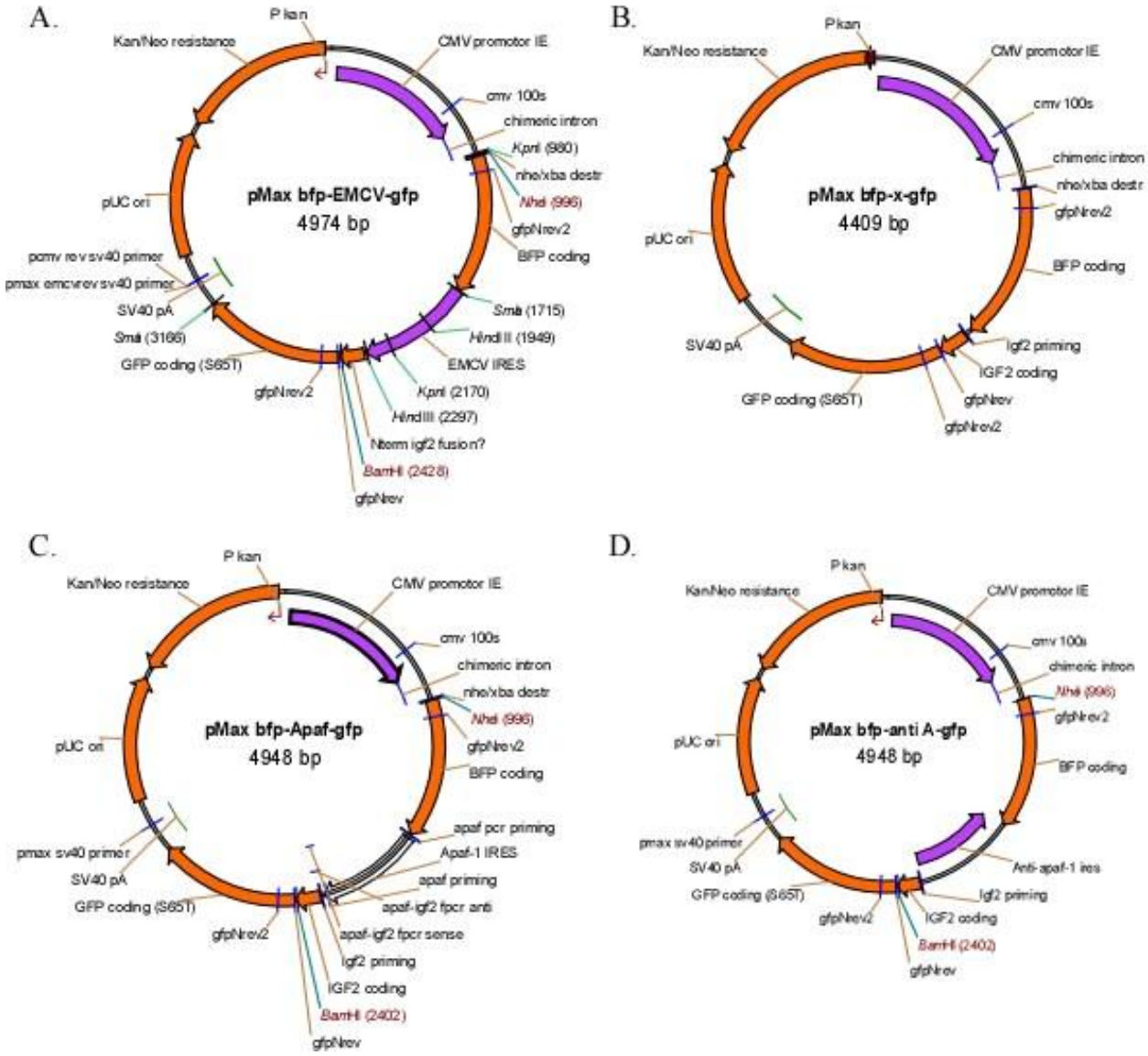

Figure 9. Bicistronic constructs (pMax plasmids). In each construct BFP is the first reporter gene upstream of the insert and GFP is the downstream reporter. GFP expression will allow quantification of any IRES activity. A. EMCV IRES (positive control) B. No IRES (negative control) C. Apaf-1 Sense IRES D. Apaf-1 Antisense IRES.

Figure 10

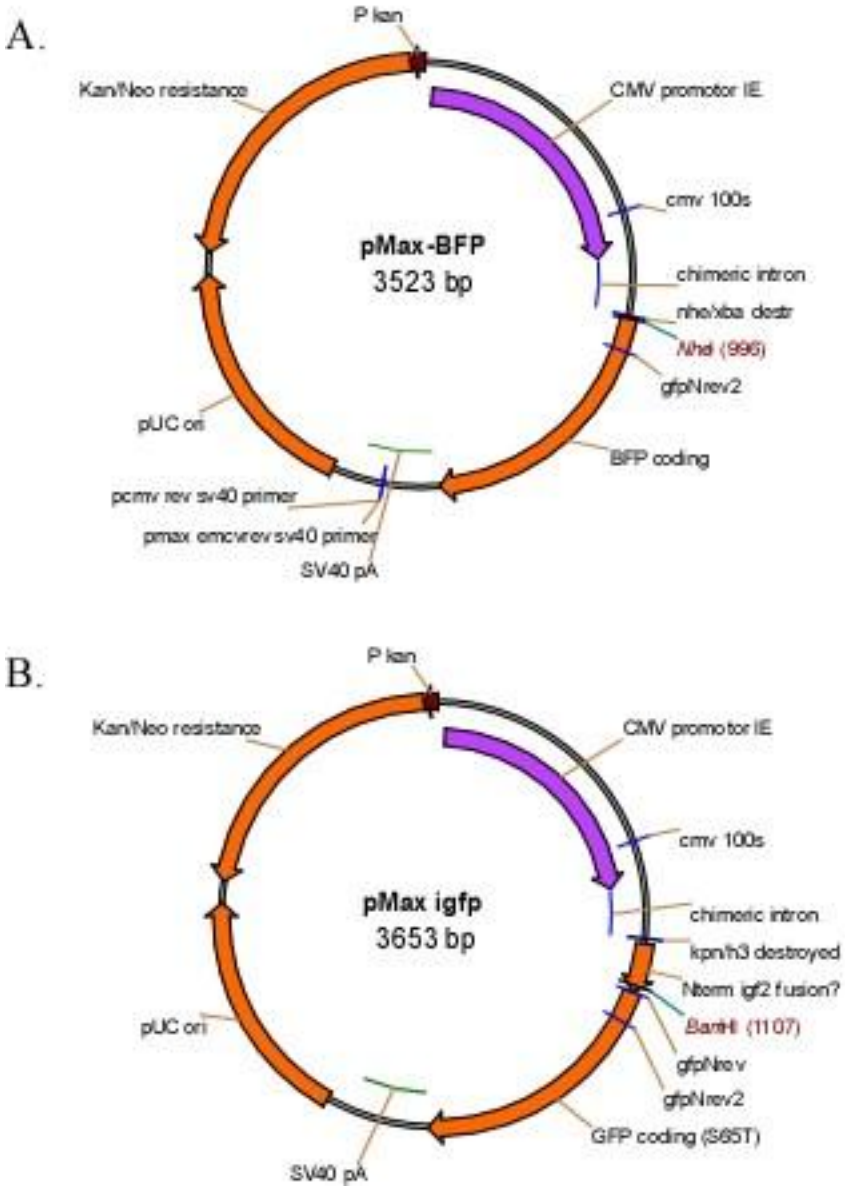

Figure 10. Monocistronic constructs (pMax plasmids). Each construct has either BFP or GFP with no IRES insert or downstream gene and are used as positive controls for each.

II. Transfection of Breast Cancer Cells with Plasmid DNA

Pilot transfections were carried out using Lipofectamie 2000 reagent. MCF10A, MCF7, T47D, and MDA-MB231 cell lines were split into 24 well glass bottom plates (MatTek) to about 200,000 cells per well in the appropriate antibiotic free medium one day prior to transfection. The plasmid DNA samples were added to Lipofectamie 2000 (Invitrogen) (1µL per reaction in a 24 well plate) in OptiMem medium (Invitrogen) and incubated at room temperature for 20 minutes. Plasmid DNA was added at a concentration of 3µg per well. The plasmid DNA was allowed to incubate with the cells for 24 hours prior to visualization with the Carl Zeiss Fluorescent microscope. Images were taken at 100X magnification for each well in three channels: DIC, DAPI (blue fluorescence), and GFP (green fluorescence) and levels of blue and green fluorescence determined using AxioVision software. Results with this protocol proved insufficient with low transfection efficiency and high numbers of cell death. A number of variations on the protocol were tried: initial cells plated were varied from 80,000/well to 200,000/well; the amount of Lipofectamine was varied from 0.5µL/reaction to 3µL/reaction; the amount of DNA was varied from 1-5µg per reaction; and plasmid DNA was EtOH precipitated for additional cleanup. Regardless of the parameters no transfection was considered to be truly successful, leading to the investigation of a new transfection method all together.

Due to inconsistent results with the Lipofectamine 2000 the transfection protocol was switched to electroporation. The preliminary transfections in MCF7 and MDA-MB231 cells tested a variety of conditions with voltage ranging from 100-250V, pulse duration ranging from 1-50ms, and pulse number from 2-5 pulses per reaction. This experiment proved more successful than Lipofectamine in the MDA-MB231 cells yielding healthy looking, fluorescing cells, but still

low in efficiency. After electroporation MCF7 cells were mostly rounded and unhealthy, therefore an early protocol was developed to optimize electroporation conditions in the MDA-MB231 cells only. This initial protocol called for cells to be concentrated to a density of $1.0x10^6$ cells/300µL media, 2 pulses at 50ms each with 100ms between pulses, and 5µg plasmid DNA per reaction. The success of this protocol was also short lived and new parameters investigated. The following protocol was arrived at following considerable optimization. This final approach gave successful and repeatable transfections with pMax-plasmids, though population efficiency remains less than 20%.

Cells were grown in T-75 flasks until ~80% confluency, and harvested using Trypsin/EDTA on the day of transfection. Cells were concentrated to a density of 2,500,000cells/mL and split into 400µL reactions ($1.0x10^6$/400 µL) in 4mm electroporation cuvettes (Genesee Scientific). 20µg of plasmid DNA was added to the reaction, and then the cuvette was placed into an ECM 830 Electro Square Porator (BTX) for pulsing. Samples were pulsed twice at 140V for 70ms each, 100ms between pulses. After pulsing, 1mL of media (10% FBS) was added to the cuvette, and the entire contents was transferred to a 24 well glass bottom plate. Cells were incubated for 24 hours prior to imaging.

a. Microscopy and Image Acquisition

Using the Carl Zeiss Axiovert 200M fluorescence microscope, positively transfected cells were identified and the microscope was set up for imaging. Images were taken at 100X magnification for each positive cell in three channels: DIC (grey channel), DAPI (blue fluorescence), and GFP (green fluorescence). Prior to imaging, the optimal exposure time was measured by the camera in each channel for the individual cell. Using the measured exposure as

a base, 4 additional exposures were chosen above or below. A total of 5 images were taken using the designated exposure times for that individual cell. With each new positively identified cell a new optimal exposure time and additional exposures were established prior to imaging.

b. Image Analysis and Fluorescence Quantification

Images were analyzed using Axiovision 4 software. To do so, a region of interest (ROI) was established by outlining the transfected cell on the digitally acquired images that overlap for all fluorescence and white light images (DIC). Once outlined, a data table was created giving the area of the cell (μm^2) and the average density output within the ROI for each of the three channels (DIC, DAPI, GFP); the table was exported into Microsoft Excel. Once in Excel, the average density output was normalized to exposure time for each image in the blue and green channels, and a ratio of green fluorescence (GFP) to blue fluorescence (BFP) was determined using the normalized value (Table 4). The [GFP/BFP] ratio was multiplited by a factor of 100 and averaged between cells transfected with the same plasmid and compared to the average density ratio of cells transfected with other pMax plasmids.

Table 4. Example calculation from a positive MDA-MB231 cell transfected with pMax-Apaf-1 Sense.

		BFP					GFP			
	Exposure Time (ms)	Density	Density/ time			Exposure Time (ms)	Density	Density/ Time	Ratio [GFP/BFP]	Ratio *100
1	1050	772.42	0.736		1	16000	520.85	0.033	0.044	4.43
2	1250	910.10	0.728		2	18000	532.71	0.030	0.041	4.06
3	1450	1045.60	0.721		3	20000	567.87	0.028	0.039	3.94
4	1650	1176.62	0.713		4	22000	548.28	0.025	0.035	3.49
5	1850	1304.16	0.705		5	24000	530.97	0.022	0.031	3.14
								Average:	0.038	3.81
								St Dev.	0.005	0.50

c. Linear Range Determination for Fluorescence Measurements: Mono- and Bicistronic pMax Plasmids

Transfections were carried out following the protocol from *Transfections of Breast Cancer Cells with Plasmid DNA* in MCF7, T47D, and MDA-MB231 cell lines for the monocistronic experiment, and MDA-MB231 for the bicistronic experiment. Using the Carl Zeiss Fluorescent microscope positively transfected cells were identified, and the optimal exposure time was measured for each of the 3 channels. Based off the measured exposure, time 7 additional exposure times were chosen, above and below the optimal point, and images were taken at 100X magnification. A ROI was established in each image, and the data tables created were exported into Microsoft Excel.

Results

I. Linear Range Determination: Monocistronic BFP and GFP constructs

In order to determine any potential signal overlap between the BFP (blue) and GFP (green) channel fluorescence signals, a range of linear response was established for each reporter protein in both the blue and green channels. In order to rely on quantification of fluorescence density relative to exposure time, we first employed monocistronic BFP and I2-GFP constructs in the parent vector, pMax, to express each fluorescent protein separately in the MDA-MB231 cell line (Figure 11). By establishing a linear relationship between these two variables for both channels, we were able to determine a consistent density output range in which to measure the primary or "correct" channel signal, as well as monitor the response in the secondary or "incorrect" channel. The fluorescence response with time (or "slope") is a measure of the

sensitivity of the camera for that wavelength of fluorescence from the given protein, GFP or BFP. In determining these responses in each channel, we found that the response of blue fluorescence by GFP can represent as much as 68% of its signal in the native green fluorescence channel. Conversely, the green fluorescence response by BFP represented considerably less bleed over into green fluorescence at 11%. To determine that 68% of the measured green signal shows up as a blue signal, the slope of the blue fluorescence by pMax-iGFP was compared to the slope of the blue fluorescence by pMax-BFP (Figure 11B). The 11% measured blue signal showing as green was determined by comparing the slope of the green fluorescence by pMax-BFP to the slope of the green fluorescence in pMax-iGFP. A linear relationship was confirmed for both BFP and GFP in the primary color channel by a R^2 value close to 1.

In an attempt to account for signal overlap in future transfections adjusted blue fluorescence (ABF) and adjusted green fluorescence (AGF) will be determined using the following calculation after the density output has been normalized to exposure time:

ABF = Blue Density/Time – ([G density/time]*[slope of B from GFP/slope of G from GFP])

AGF = Green Density/Time – ([B density/time]*[slope of G from BFP/slope of B from BFP])

G = green; B = blue

The ABF value comes from the green signal; therefore subtracting a slope ratio multiplied by the green output for a particular cell should account for signal overlap give a better representation of a true blue fluorescence output value, and vice versa for the AGF value. Unfortunately, this formula did not accurately account for background signal and an appropriate one still needs to be established. Calculations will be based solely on the density/time ratios of GFP to BFP.

Table 5. Linear Range Determination: Monocistronic. Images of positively transfected MDA-MB231 cells were taken using a series of exposure times to determine a linear relationship between exposure time and average density output.

pMax-BFP						
	BFP				GFP	
	Exposure Time (ms)	Avg Density Output			Exposure Time (ms)	Avg Density Output
1	24	83.80		1	6870	1455.50
2	124	474.59		2	7870	1543.48
3	224	862.62		3	8870	1543.94
4	324	1257.88		4	9870	1604.13
5	424	1623.91		5	10870	1628.60
6	524	2160.98		6	11870	1713.46
7	624	1975.80		7	12870	1727.63

pMax-iGFP						
	BFP				GFP	
	Exposure Time (ms)	Avg Density Output			Exposure Time (ms)	Avg Density Output
1	71	165.90		1	330	192.51
2	171	388.80		2	1030	585.17
3	271	605.40		3	2030	1107.55
4	371	822.12		4	3030	1581.74
5	471	1038.38		5	4030	1961.48
6	571	1254.40		6	5030	2311.99
7	671	1473.33		7	6030	2553.21
8	771	1694.78		8	7030	2697.19

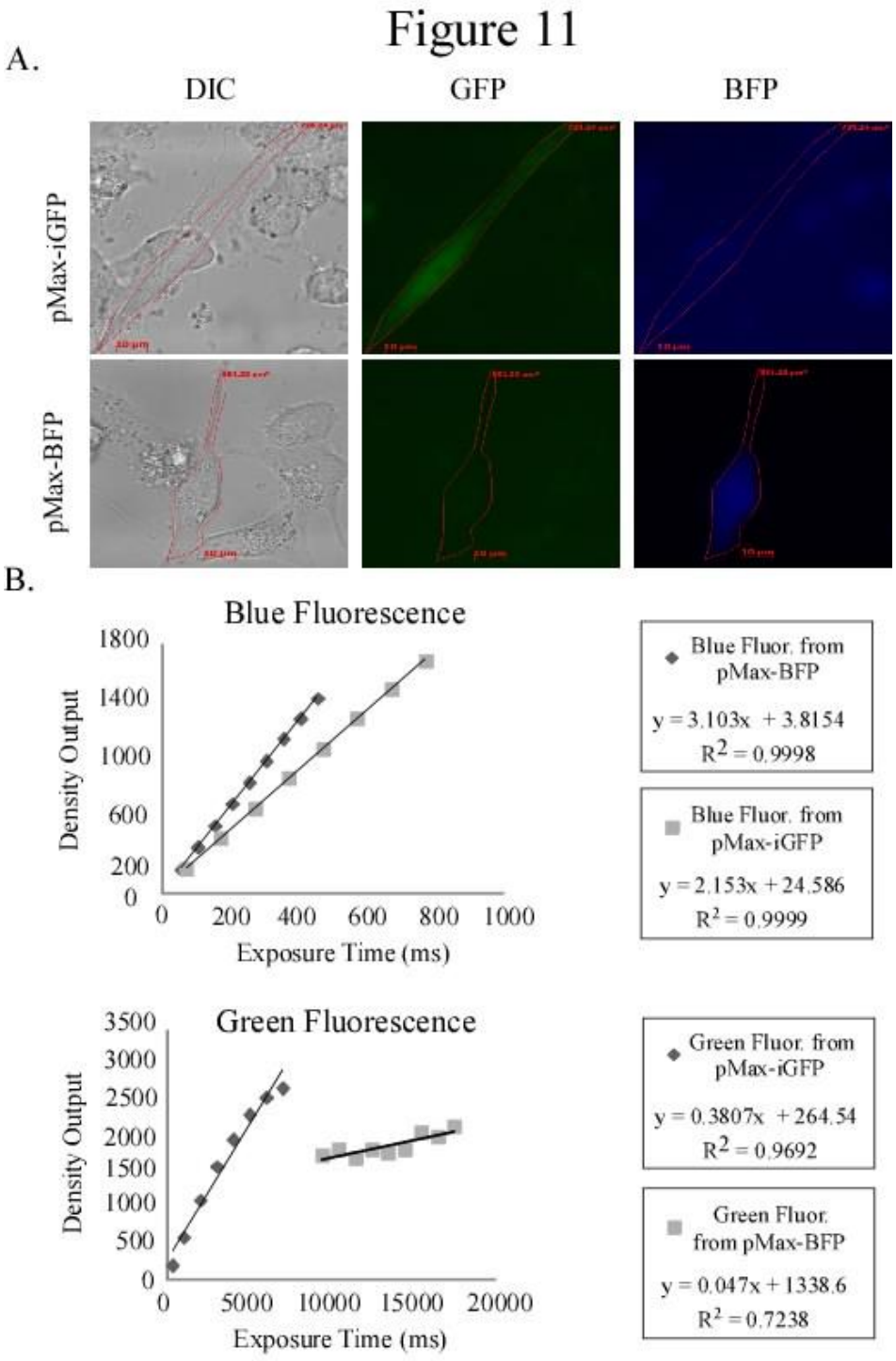

Figure 11. Linear Range Determination: Monocistronic. In each of the monocistronic pMax-plasmids the signal overlap was determined by comparing the slopes of the blue fluorescence and green fluorescence between constructs. A. Images of MDA-MB231 cells transfected with either pMax-BFP or pMax-iGFP. B. Comparing the slope of the blue fluorescence signal in each construct allowed for signal carryover to be determined in the blue channel. The same principles were used to determine green signal carryover.

II. Linear Range Determination for Fluorescence Measurements: Bicistronic BFP/IRES/GFP constructs

It was also necessary to investigate a linear relationship between exposure time and average fluorescence density output in the bicistronic pMax-plasmids containing both fluorescent protein coding regions (BFP and GFP) separated by the IRES sequence. Establishing this relationship in the bicistronic plasmids allowed us to determine an ideal density output range to use for analyzing future experimental cell treatments. In order to determine an accurate ratio of blue fluorescence (cap-dependent initiation) to green fluorescence (cap-independent initiation) it was imperative to stay within the established density output range. The EMCV IRES is a well-established and potent positive control for strong cap-independent translation. In single cells transfected with the pMax BFP/EMCV/GFP construct we found that both blue and green fluorescence were readily detectable (Figure 12). As in the monocistronic experiment, a linear relationship between exposure time and average density output was confirmed by a R^2 value close to 1 (Table 1). The average density output was normalized to exposure time, and the normalized response values used to determine the ratio of GFP/BFP. In a representative MDA-MB231 cell transfected with pMax-EMCV (Figure 12) the ratio stays consistent when the BFP and GFP channels are within an average density output range of ~500-2100 units collected by the Zeiss Axiocam camera. Above or below these values the response ratios became inconsistent. When analyzing positively transfected cells, any ROI that gives an average density output less than 500 or greater than 2100 was disregarded in the calculations.

Table 6. Linear Range Determination: Bicistronic. Example calculation of IRES activity in a representative MDA-MB231 cell positively transfected with pMax-EMCV. Establishing a linear relationship between exposure time and average density output showed a practical output range for a consistent [GFP/BFP] ratio.

	BFP					GFP				
	Exposure Time (ms)	Avg Density Output	Density/ Time			Exposure Time (ms)	Avg Density Output	Density/ Time	Ratio: [GFP/ BFP]	Ratio *100
1	4	6.65	1.66		1	300	400.91	1.33	0.804	80.38
2	14	65.86	4.70		2	600	762.85	1.27	0.270	27.03
3	64	396.50	6.19		3	900	115.65	1.24	0.200	20.01
4	114	702.68	6.16		4	1200	1408.34	1.17	0.190	19.04
5	164	986.36	6.01		5	1500	1670.03	1.13	0.185	18.51
6	214	1257.44	5.87		6	1800	1917.76	1.06	0.181	18.13
7	264	1513.34	5.73		7	2100	2119.66	1.00	0.176	17.61
8	314	1748.19	5.57		8	2300	2181.64	0.94	0.170	17.04

Figure 12

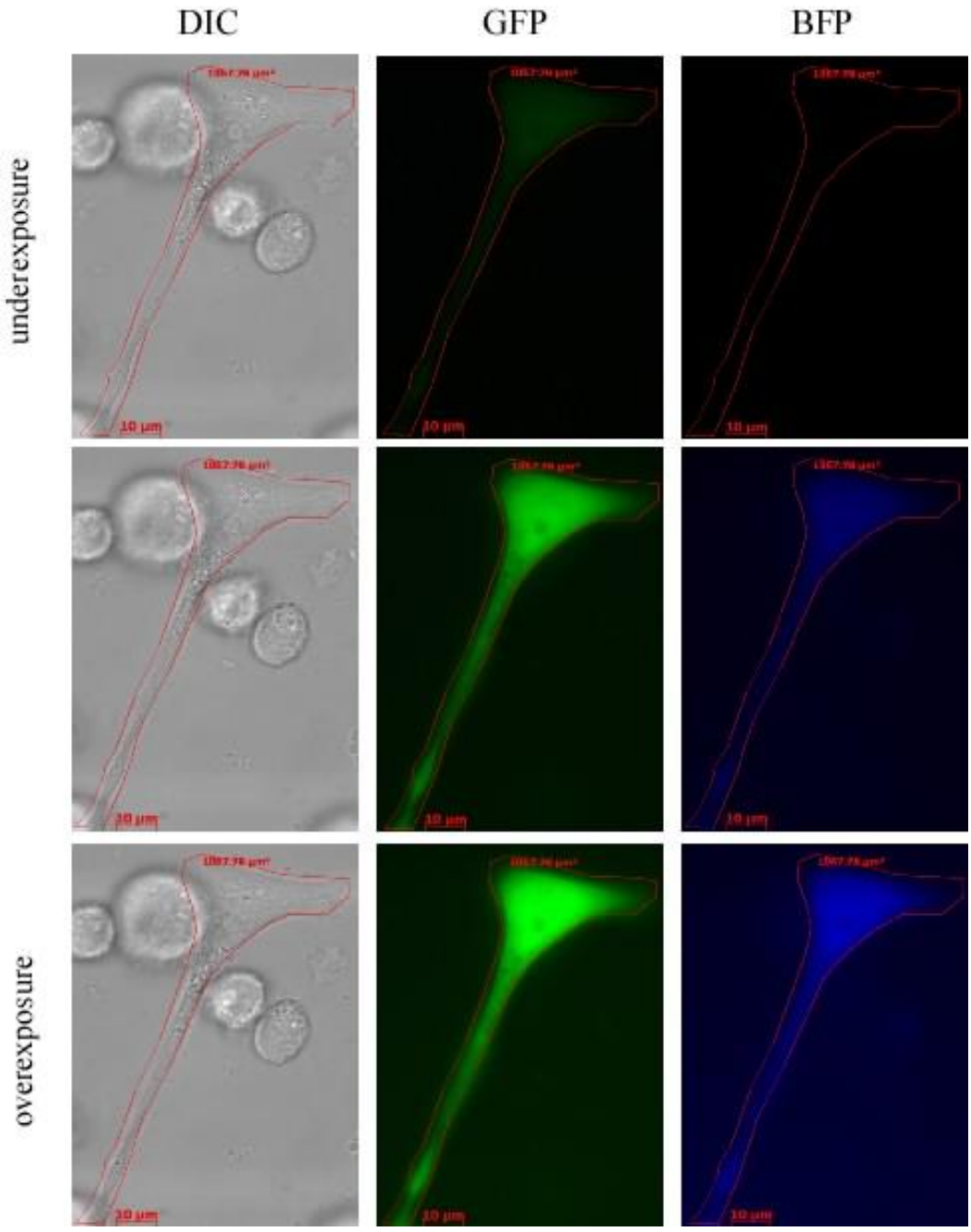

Figure 12. Linear Range Determination: Bicistronic. MDA-MB231 cells were transfected with pMax-EMCV and images taken over a series of exposure times to determine an ideal density output range for calculating IRES activities

III. Transfection of Breast Cancer cells with Bicistronic BFP/IRES/GFP constructs

Successful transfections with the pMax-plasmids allowed us to develop a method to evaluate relative levels of cap-dependent to –independent translation initiation occurring in individual lives, and eliminated the need for high efficiency transfections. Cells positively transfected with one of the four bicistronic constructs had different fluorescence patterns as expected (Figure 13). Cells transfected with pMax-EMCV showed visible fluorescence in both the green and blue channels, and required much lower exposure times in the green channel compared to each of the other constructs. This is due to the strong, constitutive expression of the second (GFP) cistron by the EMCV IRES. pMax-Apaf-1 Sense, pMax-Apaf-1 Antisense, and pMax-No IRES all had similar fluorescence patterns. Blue fluorescence was readily detected from all three constructs at relatively similar levels with exposure times averaging in the hundreds of milliseconds. Green fluorescence gave very little appreciable visible fluorescence, but the sensivity of the camera allowed measured density output readings at the low end of the required output range upon long exposures (~18 s).

After each cell was visibly assessed for fluorescence, and [GFP/BFP] ratio determined over a series of exposure times, the level of, for example, EMCV IRES activity was then evaluated between single cells in the same transfection with the same plasmid (Figure 14A). Comparisons were also made between average IRES activity ratios between experiments (Figure 14B) and total activity over a series of experiments (Figure 14C). Healthy MDA-MB231 cells showed increased IRES activity, represented by higher density outputs in the GFP channel, in only cells transfected with pMax-EMCV. The EMCV IRES, which is constitutively active, showed activity ~5x higher than that of pMax-Apaf-1-Sense or Antisense, which should only

become more active upon induction of apoptosis (Figure 14B), based on our previous experiments using a bicistronic CAT and luciferase system that measured expression post cell lysis (Blackwell 2007). Cells transfected with the plasmid containing No IRES showed activity in a similar range to Apaf-1-Sense and Antisense IRESes, confirming a basal response level from these cellular pro-apoptotic IRESes.

Figure 13

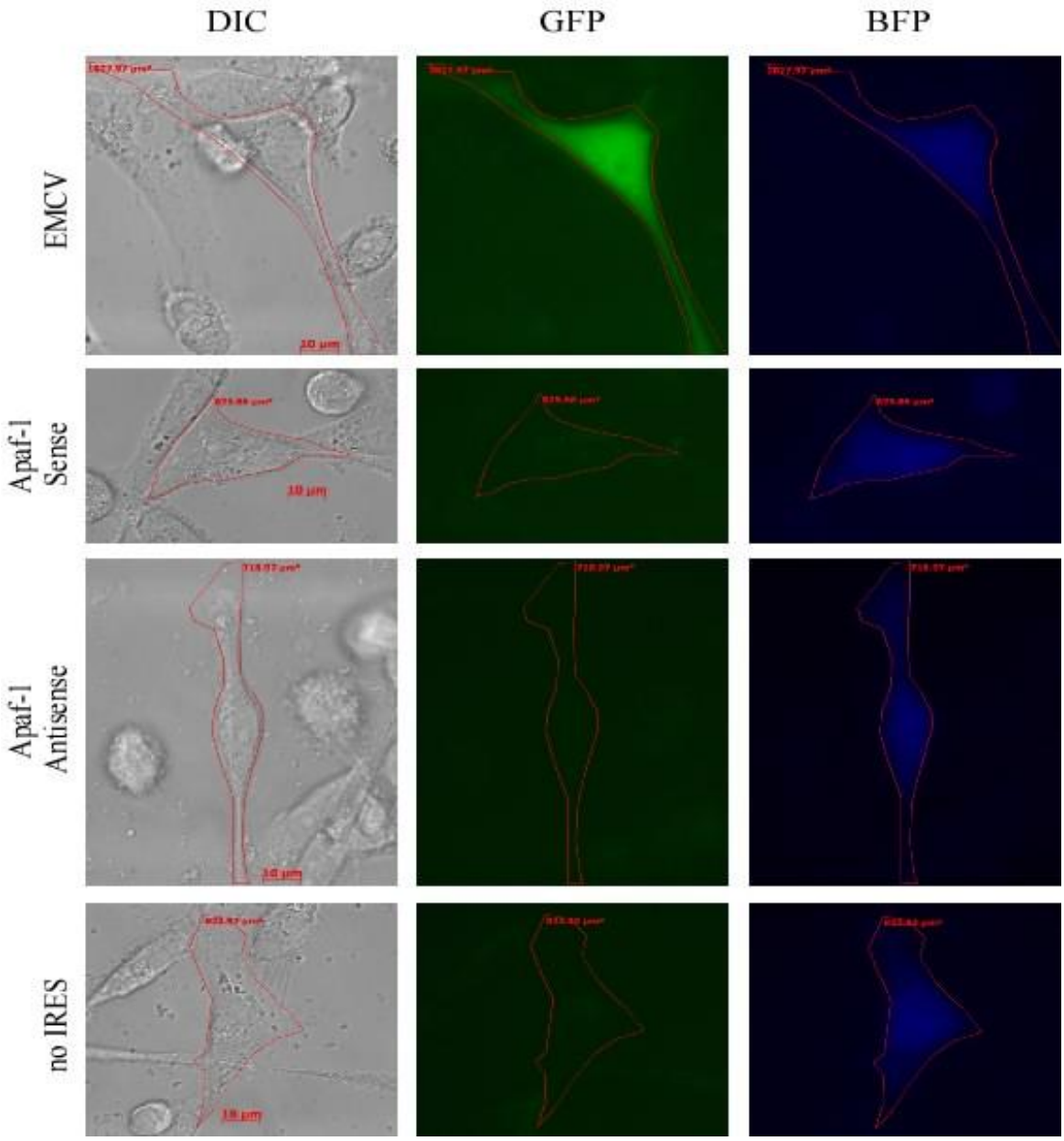

Figure 13. Relative levels of cap-dependent vs. independent translation initiation can be evaluated on a cell to cell basis. Electroporation (2-70ms pulses @140V) was used to incorporate the pMax-plasmids into MDA-MB231 cells. Representative images of a positive cell tranfected with a bicistronic plasmid are shown in each of the three image acquisition channels: DIC, GFP, and BFP. Only cells transfected with the constituently active EMCV IRES show substantial IRES activity (green fluorescence) without the induction of apoptosis.

Figure 14

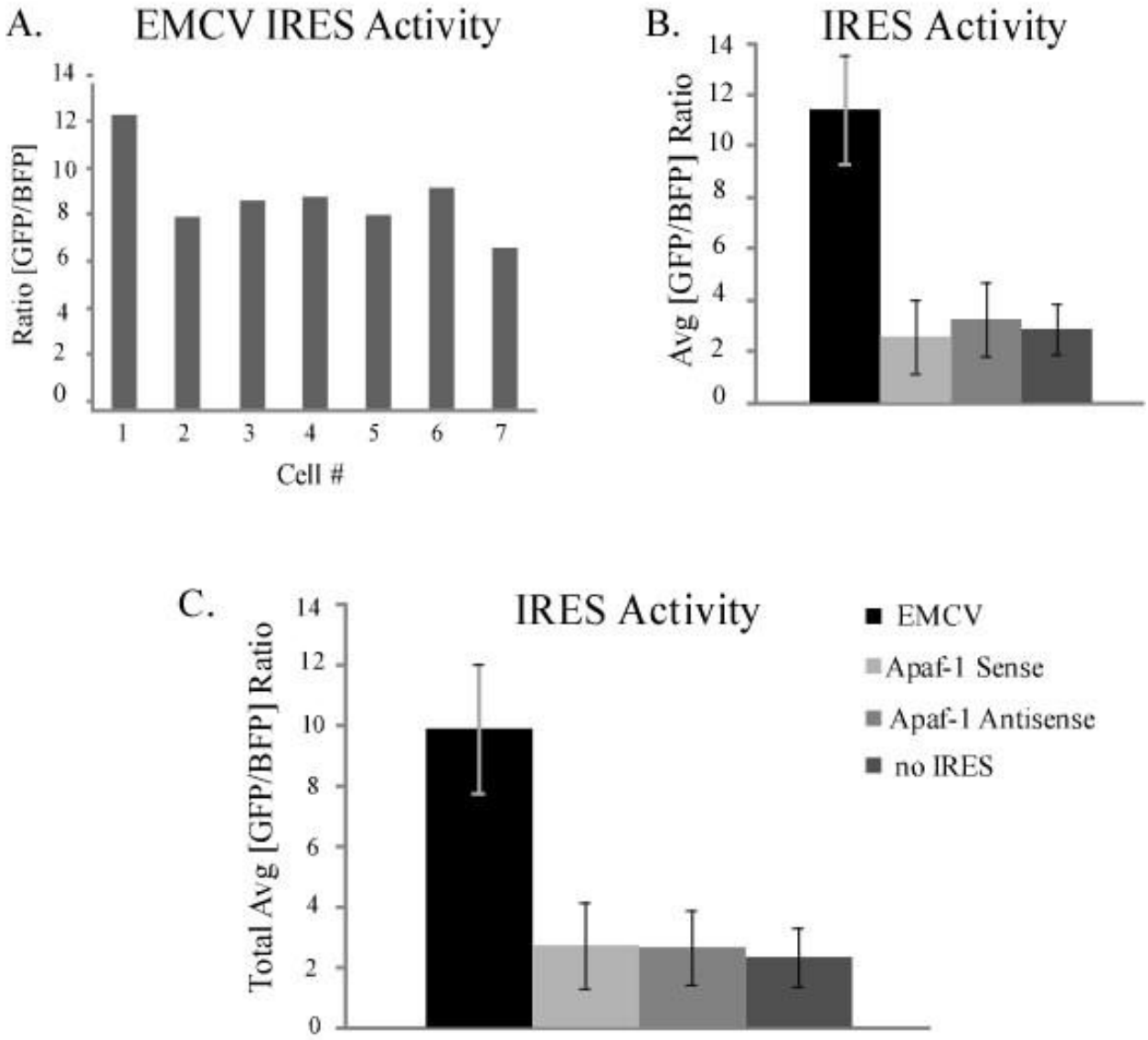

Figure 14. The activity of each IRES can be evaluated on an individual level, as well as overall activity in a given cell line. A. A comparison of EMCV IRES activity between cells in the same transfection. The same can be achieved for the Apaf-1 Sense, Antisense, and no IRES constructs. B. Comparison of all IRES activity in one experiment (N=7). C. Overall average IRES activity between multiple transfection experiments (N=3).

Discussion

Evaluating shifts in the translation initiation mechanism began with previous studies in the Keiper Lab (Blackwell 2007) using β-gal/IRES/CAT-LUC plasmid constructs. These transient transfection experiments allowed for the relative cap-dependent and –independent translation activity to be evaluated only after cell lysis and only in whole populations of MCF7 cells. This study found that when eIF4G-1 was depleted, or after treatment with etoposide or cisplatin it elicited enough cell stress to induce the Apaf-1 IRES (Blackwell 2007). While this assay allowed the rough quantification of cap-independent activity in populations of cells, it did not give information on how individual cells reacted to depletion of eIF4G-1 or drug treatment. Creation of the dual fluorescence reporter plasmids presented the possibility to develop a method to look at translation initiation mechanism shifts in single live cells and in real time during drug treatments, based directly on the intensity in expression of two distinct fluorescent proteins. The basic idea of the dual fluorescence plasmid is the same as the β-gal/IRES/CAT-LUC used in whole cell populations. Similar to the previous experiments it was expected that levels of blue fluorescence would be translated in a cap-dependent manner and express strongly across each construct, which proved true with expression levels ~5x greater than that of the control which contained no IRES. The variation came in the GFP expression which required the use of the IRES to initiate translation. Similar to the transfections in MCF7 cells without siRNA knockdown of eIF4G-1, it was expected that the induction of the EMCV IRES would give a strong response, while the Apaf-1 IRES would only be induced under apoptotic or cell stress conditions. Although eIF4G-1 depletion was not conducted in this study, the hypothesis was supported in that no real induction of the Apaf-1 IRES occurred when compared to the control in untreated cells (Figure 14C). Comparing IRES activity in the population of individual cells

versus previous experiments in whole cell populations confirms the reliability of the novel plasmid constructs in measuring relative translation initiation mechanisms.

Transfection with the dual fluorescence constructs allows for the IRES activity in individual live cells to be evaluated in real time. IRES activity can, and will, vary from cell to cell as seen in a representative population of cells transfected with the EMCV IRES (Figure 14A). Further studies using this technique could allow exploration into how associated proteins or various cell stress conditions affect a specific IRES's efficiency. Activity can also be compared in a number of IRESes over a given experiment (Figure 14B), and then again as an average over cell populations (Figure 14C). With the capabilities to look at the IRES activity in an individual cell it opens up the possibility to follow the shift from cap-dependent to – independent translation in real time by observing the induction of the IRES. Future studies will include real time assessment of the induction of the Apaf-1 IRES and the Apaf-1 Antisense IRES after treatment with etoposide and cisplatin. In this way, the kinetics of such a response in conjuction with the induction of, for example, DNA damage or caspase activation can also be assessed. The Apaf-1 antisense IRES is expected to act as a negative control, and not yield significant green fluorescence. However, there is a possibility that secondary structures associated with the complementary IRES sequence could recruit ribosomes and initiate some translation as previously seen in work done in MCF7 cells depleted of eIF4G-1(Blackwell 2007). Alongside monitoring the induction of the Apaf-1 IRES, the opposite could also be observed. Cells could be pushed into an apoptotic state indicated by an active Apaf-1 IRES, and then conditions that might reverse the IRES activity could be investigated. Using this innovative method for individual live cell assessment will allow a deeper understanding of what type of translation initiation is predominating in a diverse group of cell types and environmental factors.

Objective 3: Response of Breast Cancer Cell Lines to Chemotherapeutic Agents

Introduction:

Chemotherapy treatments are often used to inhibit growth and eliminate breast cancer. Etoposide and cisplatin are two commonly used chemotherapy drugs, both of which are known to induce apoptosis in cells. Etoposide creates single and double stranded DNA breaks to arrest cell cycle, and cisplatin causes nuclear lesions and DNA crosslinks which ultimately lead to cell death (van Maanen, RetÃ¨l et al. 1988 ; Siddik 2003; Alderden, Hall et al. 2006). After induction of apoptosis by treatment with etoposide or cisplatin we wanted to investigate any shifts in eIF4G isoform representation and p97 levels, as well as any changes in the ratio of cap-dependent to cap-independent translation through the Apaf-1 IRES. Evaluating shifts in isoform trends or IRES activity could help link certain eIF4G isoforms to apoptosis, and give better insight on manipulating a cell's fate towards cell death.

Materials and Methods:

I. Dose Response Curve

T47D cells were plated in triplicate at a density of 100,000 cells per mL in RPMI Complete medium in 35mm tissue culture dishes (Corning). 48 hours after plating, cells were treated with concentrations ranging from 10μM-40μM of etoposide, cis-platin, or no treatment (DMSO). Upon treatment cells were incubated at 37°C for 24 hours. Cells were harvested using Trypsin/EDTA and living cells counted using Trypan blue exclusion assay to determine an adequate treatment dose.

II. Drug Treatment Time course

T47D cells were seeded in triplicate a density of 200,000 cells per mL in 2mL of RPMI Complete medium in 35mm tissue culture dishes (Corning). 48 hours after seeding cells were either left untreated, treated with etoposide [40 μM], or treated with cis-platin [30 μM]. Cells were harvested using Trypsin/EDTA, and living cells counted using Trypan Blue exclusion upon initial treatment. This was repeated every 8 hours for 72 hours total to determine the appropriate time to harvest cells for protein lysates.

III. Treatment of Cells for Protein Lysates and Western Blotting

Cells were grown in a T-75 cell culture flask in appropriate medium until ~60-70% confluency. Cells were then treated by adding either etoposide or cis-platin to the media at a concentration of 30μM or 40 μM, respectively, for 48 hours. The cells were harvested using Trypsin/EDTA and lysed following the same procedure as *Preparation of Cell Lysates*.

Results

I. Dose Response Curve

A dose response was carried out in T47D cells using both etoposide and cisplatin in order to determine an appropriate level of treatment. Viable cells were counted after 24 hours of treatment using Trypan blue and the cells/mL determined using the following formula:

$$\text{cells/mL} = (\text{total cells counted}/8)(2)(10{,}000)$$

The number of viable cells/mL was graphed versus concentration in Microsoft Excel, and analyzed for approximately 50% killing (Figure 15). T47D cells were chosen because they,

unlike the MCF7's, have a functional caspase-3 gene therefore apoptosis should be readily induced, and they represent our mid-range in terms of 'aggressive' behavior. A concentration of 40μM was chosen for etoposide and 30 μM for cisplatin as the level of treatment for further experiments. These concentrations allowed for approximately 50% killing from the control treatment, which shows cells are clearly entering apoptosis, but leave enough living cells to harvest for protein lysates.

Figure 15

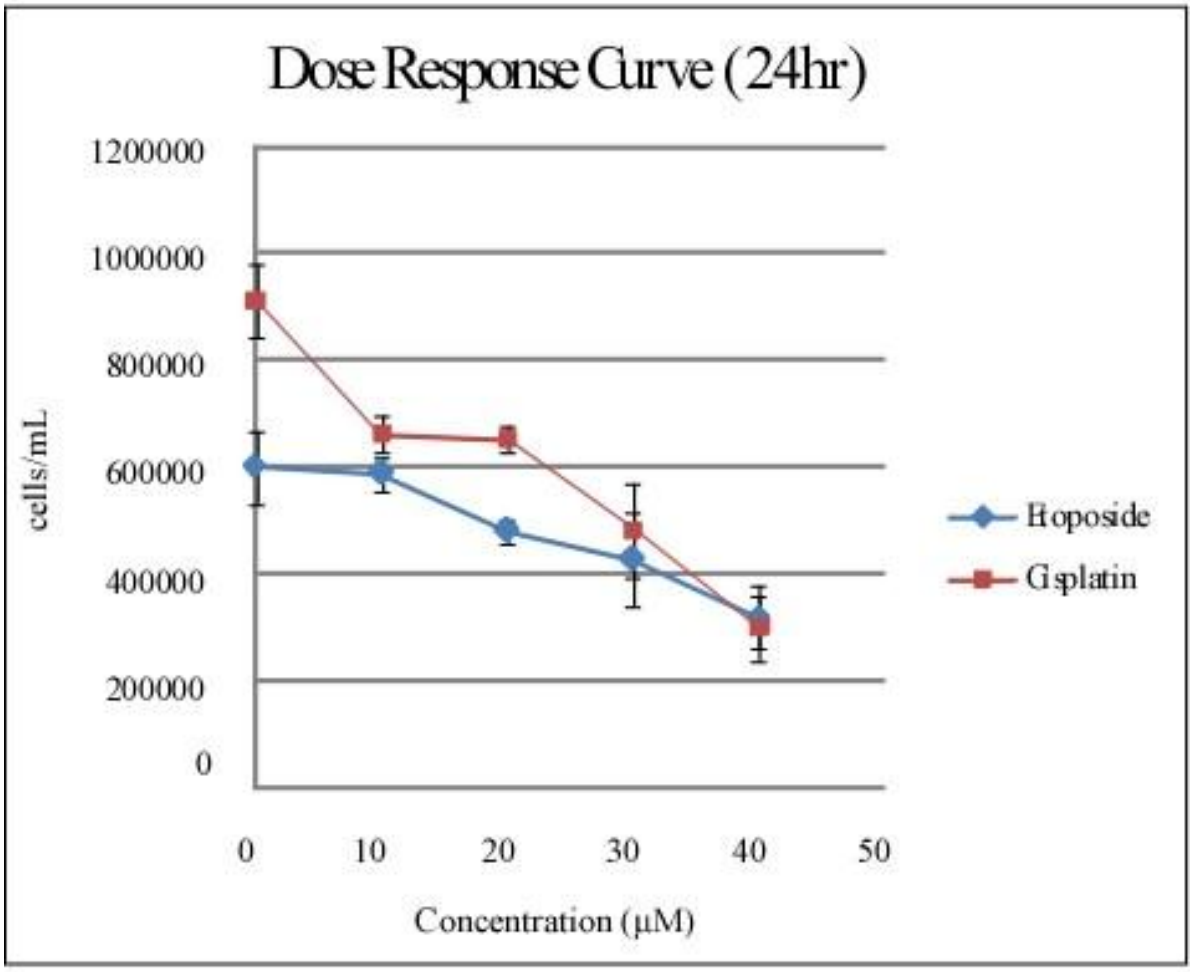

Figure 15. Dose Response Curve for cell killing by etoposide and cis-platin in T47D cells. Cells were treated with either etoposide or cisplatin for 24 hours at concentrations ranging from 0-40µM and living cells counted using Trypan blue

II. Drug Treatment Time-course

After the level of treatment was determined for both chemotherapy drugs a treatment time-course was needed to determine the appropriate time to harvest cells for lystates. Cell numbers were determined using Trypan blue, cells/mL calculated using the formula from *Dose Response Curve*, and then graphed in Microsoft Excel. The T47Ds treated with either etoposide [30μM] or cisplatin [40μM] showed approximately 50% killing after 48 hours. Although there is an initial dip in cell number at 8 hours, it's not significant enough to be confident the majority cells are shifting towards cell death, and could be attributed to plating discrepancies. To make treated lysates cells will be incubated for 48 hours with the chemotherapy drug which should allow enough time for cells to enter apoptosis while leaving enough living cells to harvest for protein analysis.

Figure 16

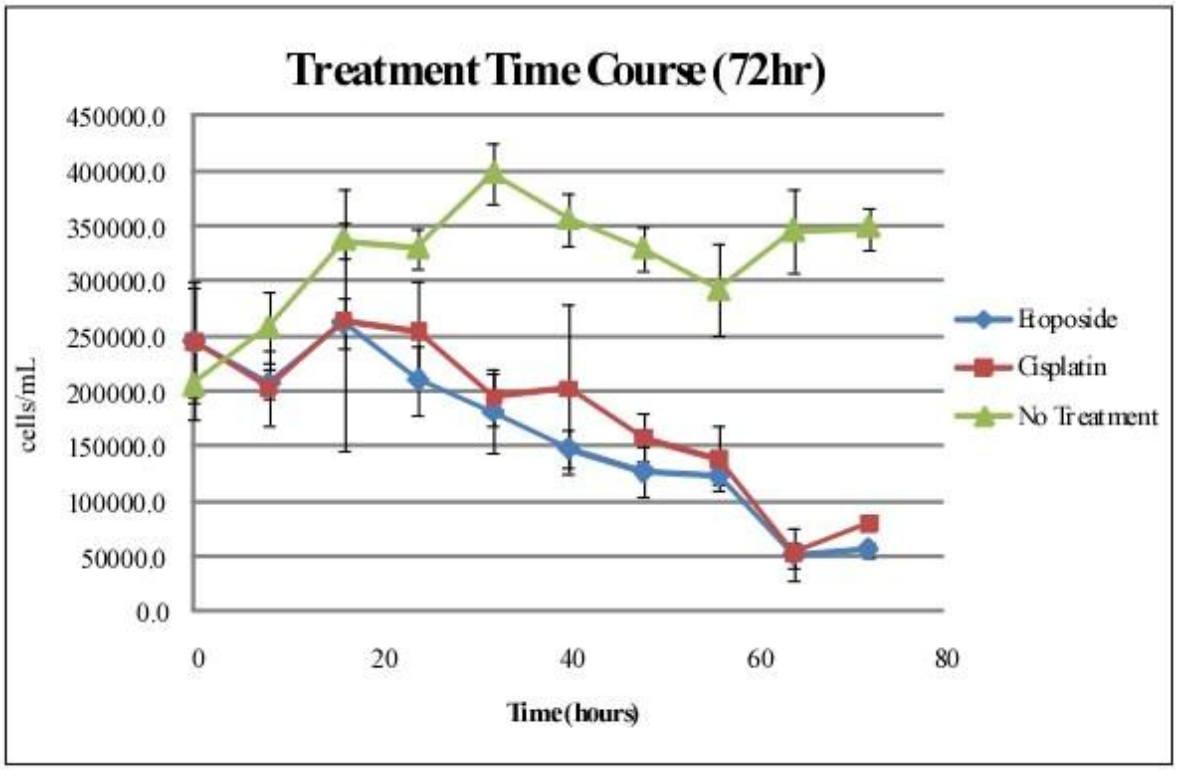

Figure 16. Drug Treatment Time Course. T47D cells were treated with etoposide [30µM], cisplatin [40µM], or left untreated, and viable cells counted using Trypan blue in 8 hour increments for 72 hours. ~50% killing was accomplished at 48hours

III. Variations in eIF4G-1 Isoforms After Treatment with Chemotherapy Agents

Upon the induction of apoptosis eIF4G-1 is cleaved and begins to act as a positive feedback regulator for IRES mediated translation initiation (Keiper, Gan et al. 1999). Immunobloting of total protein lysates from cells treated with the chemotherapy drugs etoposide, or cisplatin, were used to investigate any shifts in eIF4G-1 isoform abundance upon the start of apoptosis. MCF10A cells were not used in any treatment experiments due to their slow growth phenotype and markedly higher sensitivity to chemotherapy drugs in the concentration range used here. Lysates from MCF7 cells upon treatment showed relatively consistent isoform abundance regardless of drug type. High resolution SDS-PAGE and immunoblotting for eIF4G-1 isoforms did not give an indication that treatment had a noteworthy effect on the isoform abundance or relative representation (Figure 17A). The average percent isoform representation measured by ECL+ fluorescence quantification supported this visual estimation, except in the longest isoform, f. Cisplatin treatment, when compared to untreated lysates, showed a significant decrease in the percent representation (Figure 17B). Furthermore, isoform a, the smallest, showed an increase in representation when treated with cisplatin when compared to untreated cells, but was not found to be statistically significant. Trends in eIF4G-1 isoform alteration, if any, are quite moderate.

T47D lysates treated with chemotherapy drugs showed similar results to MCF7 cells. Resolution of eIF4G-1 isoforms by SDS-PAGE indicated a similar abundance pattern (Figure 18A), and the percent isoform representation showed no significant difference between treated and untreated isoform abundance except for isoform c. In cells treated with etoposide, isoform c abundance is markedly higher than in those cells left untreated (Figure 18B). While not a

significant difference, there are also decreased levels of isoform f and a in cells treated with etoposide versus untreated. A similar trend in eIF4G-1 isoform alteration has been seen before by Coldwell and Morley (Coldwell and Morley 2006). After depletion of eIF4G-1 isoforms by siRNA, f and a were most significantly decreased, while isoform c remained constant indicating that isoform c was capable of maintaining cap-dependent translation initiation (Coldwell and Morley 2006). An increase in isoform c after treatment may be a final attempt at maintaining cap-dependent initiation and avoiding apoptosis. Differences in MCF7 cells and T47D cells between each specific treatment were also evaluated (Figure 19). Regardless of treatment type, MCF7 and T47D isoform representations were comparable, suggesting that these "aggressive" breast cancer cell lines maintain eIF4G-1 isoform levels similarly when challenged by chemotherapeutic agents. Lysates from MDA-MB231 treated cells were also prepared, but protein extracts were routinely unable to be resolved by SDS-PAGE for reasons unknown.

Figure 17

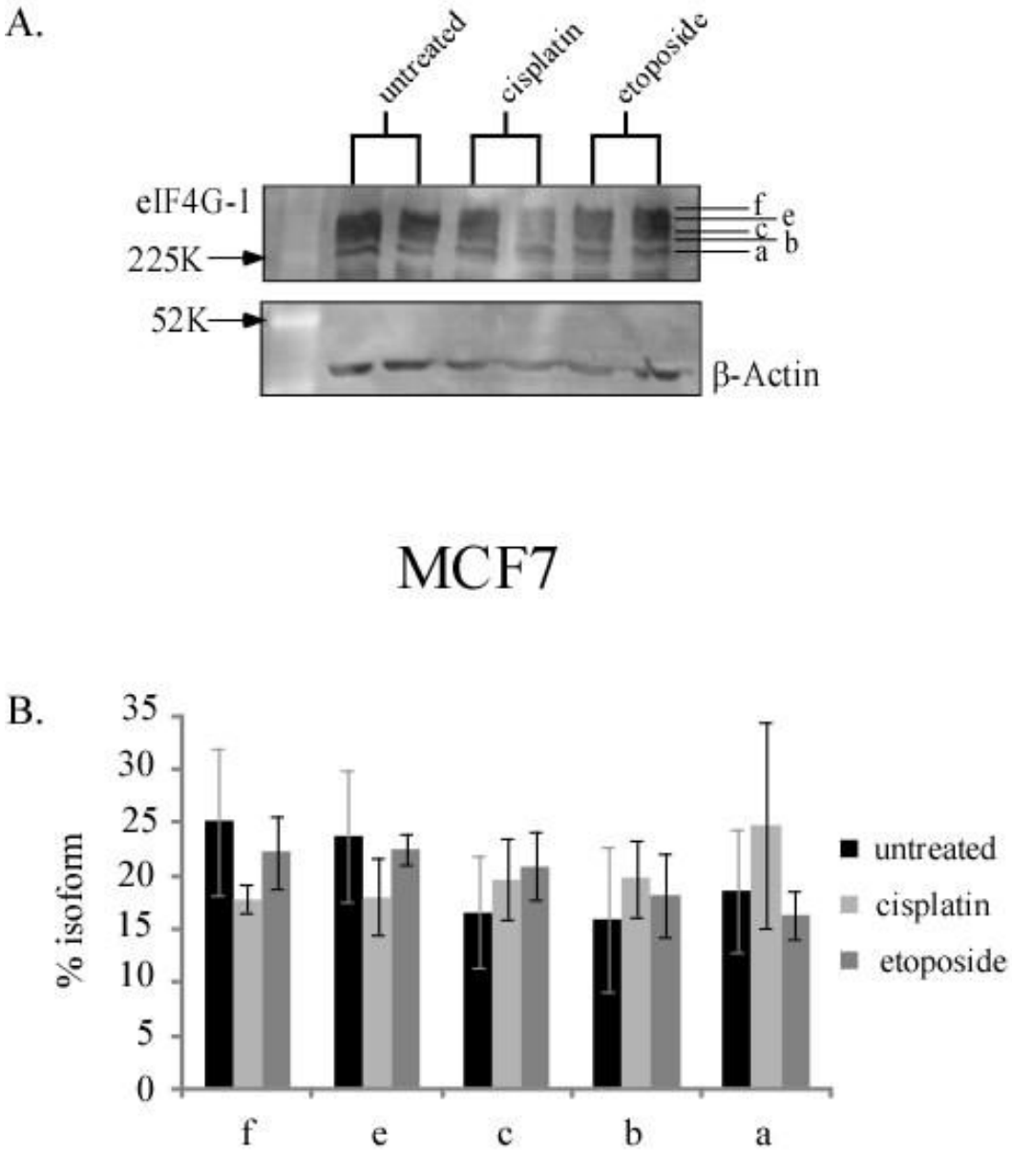

Figure 17. eIF4G-1 isoform variations in MCF7 cells treated with chemotherapy drugs. A. Western blot analysis of eIF4G-1 isoforms in MCF7 cells treated with cisplatin, etoposide, or left untreated. Cells were harvested for lysates at ~60% confluency and samples were run on a 5% (38:1) SDS-PAGE gel and probed with α-ZPI (eIF4G N-term) pAb (1:2000). Longest isoform variation is labeled as f, shortest as a. B. % isoform representation in treated lysates. Error derived from standard deviation (untreated N=12; treated N=2). * denotes p-value < 0.05 compared to untreated.

Figure 18

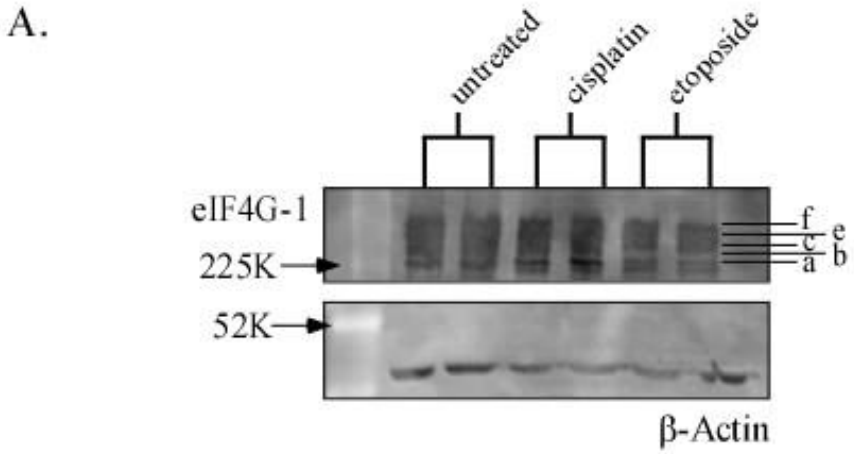

T47D

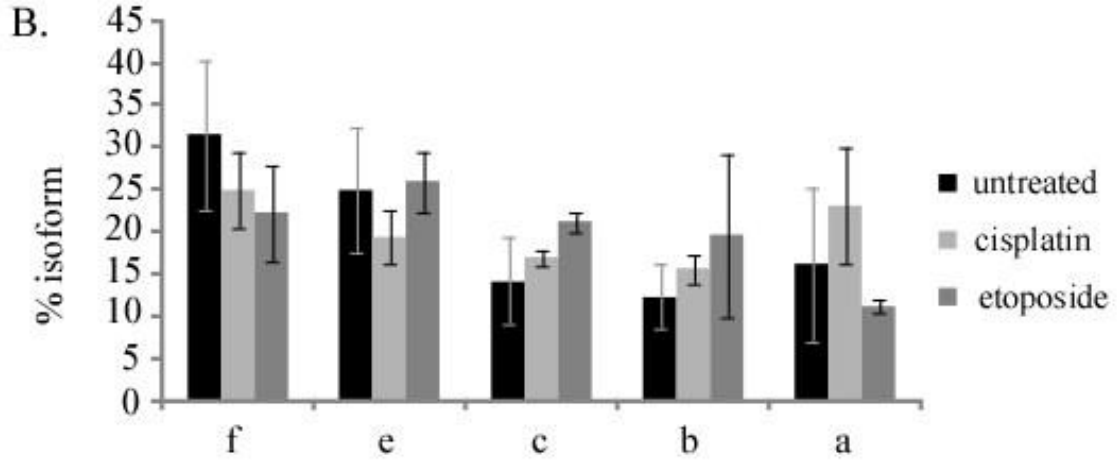

Figure 18. eIF4G-1 isoform variations in T47D cells treated with chemotherapy drugs. A. Western blot analysis of eIF4G-1 isoforms in T47D cells treated with cisplatin, etoposide, or left untreated. Cells were harvested at ~60% confluency and samples were run on a 5% (38:1) SDS-PAGE gel and probed with α-ZPI (eIF4G N-term) pAb (1:2000). Longest isoform variation is labeled as f, shortest as a. B. % isoform representation in treated lysates. Error derived from standard deviation (untreated N=12; treated N=2). * denotes p-value < 0.05 compared to untreated

Figure 19

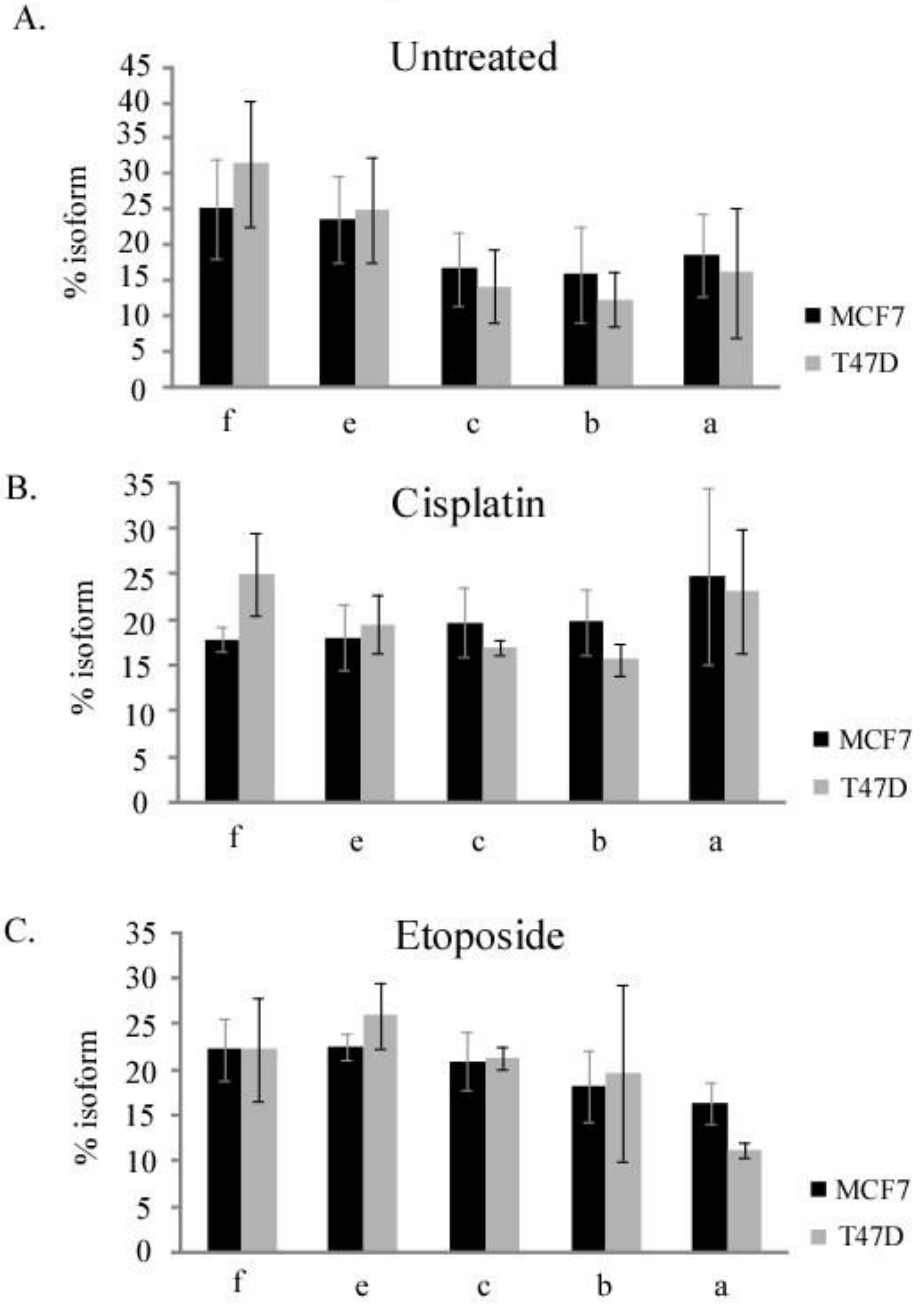

Figure 19. eIF4G-1 isoform variations between MCF7 & T47D cells treated with chemotherapy drugs. A. % isoform representation in untreated lysates. B. % isoform representation in cisplatin treated lysates. C. % isoform representation in etoposide treated lysates.

IV. Variations in p97 Levels After Treatment with Chemotherapy Agents

Total protein lysates described above from cells treated with etoposide or cisplatin were also analyzed for changes in p97 levels as compared to untreated lysates. Upon the initiation of apoptosis, caspase-3 activation results in p97 being cleaved at its C-terminal to create the p86 fragment, which in turn initiates translation of its own mRNA in an IRES dependent manner (Henis-Korenblit, Strumpf et al. 2000). Immunoblotting showed a distinct band at ~97kDa with decreasing abundance of p97 in those samples treated with either etoposide or cisplatin across all cell lines (Figure 20A, B, C). Cisplatin treatment caused a significant decrease in MCF7 and T47D cells, with p97 levels ~4x and ~2.5x lower, respectively (Figure 20D). While p97 levels were similar in MDA-MB231 cells treated with cisplatin these cells had a lower initial abundance overall. Alternatively, etoposide treatment did cause a significant decrease in p97 in MDA-MB231 cells as well as T47D cells (Figure 20D). MDA-MB231 cells showed ~3.5x decrease in p97 and T47D cells even more significant at ~8x decrease compared to the abundance in untreated protein lysates.

Detection of p86 requires immunoblotting with an antibody specific to the N-terminal portion of p97 due to cleavage of the C-terminal by caspase-3 (Henis-Korenblit, Strumpf et al. 2000). In conjunction with the initial antibody specific to aa 672-830 (C-term) (BD Transduction Labs) which detects intact p97, immunoblots with an antibody specific to an area surrounding aa 450 (N-term) (Cell Signaling) was used to detect p86 in the same treated protein lysates. Unfortunately, in our hands immunoblotting with this antibody did not allow specific p86 detection and resolution. Bands consistent with p86 migration could not be distinguished from non-specific binding of similarly sized fragments (data not shown). Regardless, a significant decrease was seen in the abundance of p97 in cells treated with chemotherapy drugs

indicating cleavage of p97 and, presumably, the activation of IRES mediated translation initiation as has been demonstrated by others.

Figure 20

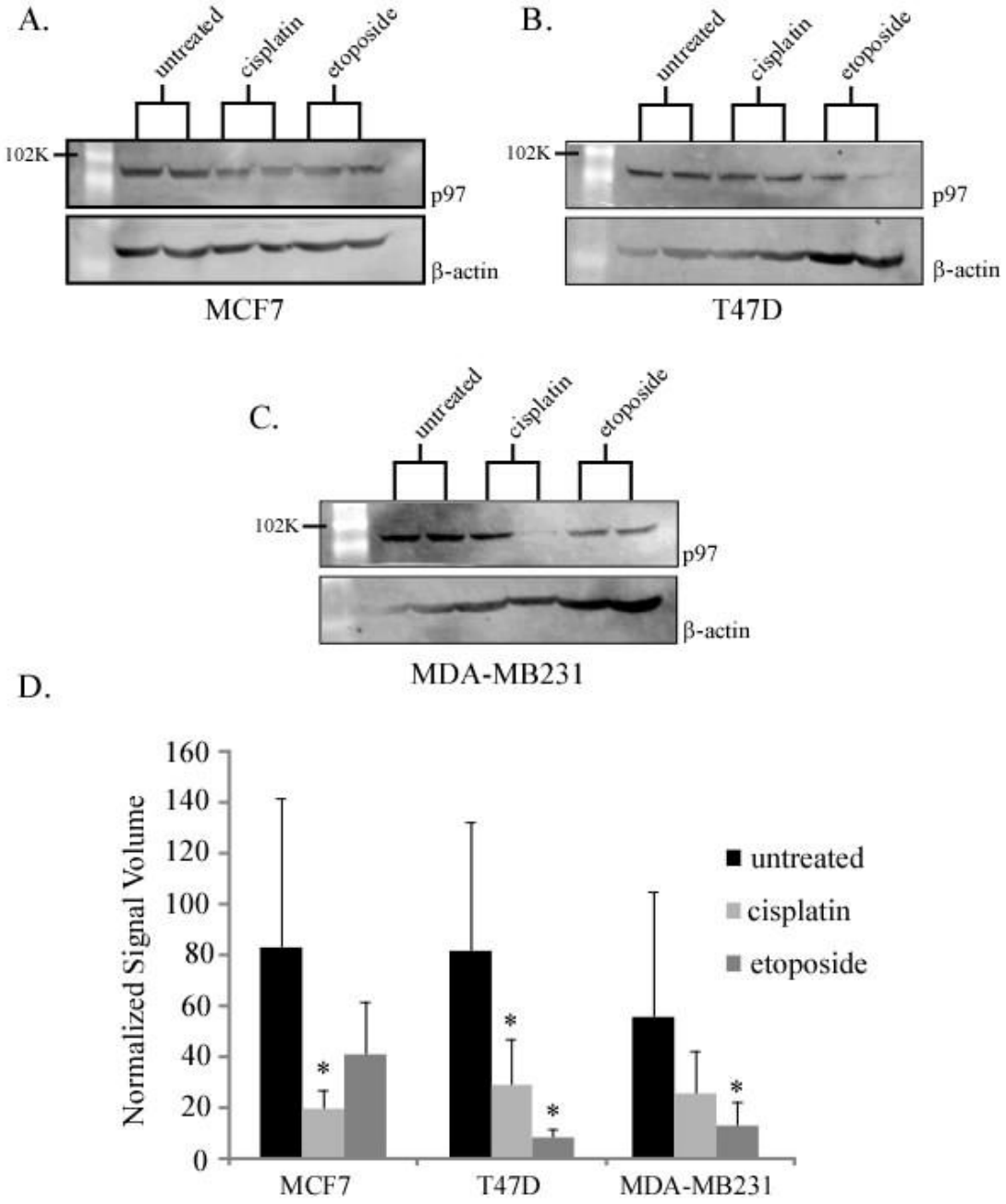

Figure 20. Variations in p97 levels after treatment with chemotherapy drugs. Cells were treated with cisplatin, etoposide, or left untreated. A. Western blot analysis for p97 in MCF7 cells run on a 10% (38:1) SDS-PAGE and probed with α-NAT1 (p97) mAb (1:1000). (kDa = 97). B. Western blot analysis in T47D cells. C. Western blot analysis in MDA-MB231 cells. D. Normalized p97 levels in cells left untreated (N=9), treated with cisplatin (N=4), or treated with etoposide (N=4). * denotes p-value < 0.05 compared to untreated lysates.

Discussion

It has been well established that the chemotherapy drugs etoposide and cisplatin are effective in attacking cancerous cells by inducing apoptosis (Cox, Burton et al. 1989; Siddik 2003). In doing so, they elicit a protein synthesis shift within the cell to translate subsets of proteins that will favor first cell survival (resistance), then later apoptosis, with the major player in this shift being eIF4G-1 (Holcik and Sonenberg 2005). With this in mind it was surprising to find that upon treatment with etoposide or cisplatin there was little significant change in the representation of "long" eIF4G-1 isoforms compared to untreated protein lysates. In MCF7 cells this could be attributed to their caspase-3 deficiency. Caspase-3 is responsible for a number of events that lead to cell death, such as DNA fragmentation, blebbing, and amplification of apoptotic signals. In a study by Blanc et. al, the authors found that until caspase-3 was transfected into MCF7 cells, they were unresponsive to cisplatin treatment as indicated by the lack of key cell death events (Blanc, Deveraux et al. 2000). Similar results were seen when MCF7 cells were treated with etoposide. No nuclear or DNA fragmentation was detected after treatment until after the caspase-3 gene was successfully restored in the cells (Yang, Sladek et al. 2001). The insensitivity of MCF7 cells to chemotherapy drugs would suggest a similar isoform profile pattern to that of untreated cells since apoptosis is not being readily induced.

T47D cells do have a functional caspase-3 gene, but still show little variation to treatment with chemotherapy drugs compared to untreated samples in our studies. The isoform abundance of topoisomerase II in these cells could attribute to their insensitivity to etoposide upon treatment. Topoisomerase II, a target of etoposide, exists in 2 forms, α and β. Houlbrook et. al, were able to show that cells containing more of the toposiomerase IIβ isoform were more

sensitive to etoposide treatments than their IIα counterparts. Of the six cell lines tested, T47D's ranked 4th in terms of IIβ isoform abundance (Houlbrook, Addison et al. 1995) indicating insensitivity to etoposide treatment. Future studies should include a more effective means of treating each cell line with chemotherapy reagents to establish a more complete isoform profile. There may be a physiological connection between the DNA damage response in T47D cells and the cleavage of eIF4G-1 by caspase-3 that has yet to be explored.

p97, the eIF4G homolog which lacks the eIF4E binding site, showed some significant decreases after treatment with chemotherapy drugs. p97 is a caspase-activated protein that when cleaves forms the protein p86 (Henis-Korenblit, Strumpf et al. 2000). Therefore, it is not surprising that each cell line showed a significant decrease in p97 levels after treatment with etoposide, cisplatin or both. Although MCF7 cells lack a functional caspase-3 gene, the activation of p97 could be by other effector caspases such as caspase 6 or 7 (Yang, Sladek et al. 2001). This decrease in p97 and subsequent increase in p86 gives a good indication that a shift in the mode of translation initiation is occurring in these cells.

While p86 may promote cap-independent translation initiation it does not necessarily indicate a decided cell death fate. Previous studies have shown that p97/p86 drive IRES mediated translation initiation both in vitro and in vivo for proteins that are both pro- (XIAP) and anti-apoptotic (Apaf-1, p97 itself) (Henis-Korenblit, Strumpf et al. 2000; Nevins, Harder et al. 2003). This may be why significant changes can be seen for p97, but not for eIF4G-1 isoforms, upon treatment with etoposide or cisplatin. Sherrill et. al was able to show that upon treatment of 293T kidney cells with etoposide or cisplatin 4E-BP1 was dephosphorylated, interrupting cap-dependent translation initiation, before apoptosis became evident in the cells. By doing this, the cells were promoting the translation of Bcl-2 using its IRES and delaying cell death (Sherrill,

Byrd et al. 2004). If a similar occurrence is taking place in MCF7 and T47D cells then an increase in p97/p86 while maintaining a constant isoform representation would not be unexpected. Overall, translation initiation by p97/p86 allows for fast, temporary up-regulation of pro- and anti-apoptotic proteins to maintain the balance between cell survival and cell death (Morley, Coldwell et al. 2005).

Conclusion:

In conclusion, we observed that across four breast cancer cell lines eIF4G-1 isoforms have similar representations, contrary to the hypothesis. The longer isoforms of eIF4G-1 are more abundant most likely due to their interactions with eIF4E and PABP which play a role in cap-dependent translation initiation. Upon treatment of the breast cancer cells with chemotherapy drugs similar results were seen, which could be attributed to the cell favoring synthesis of anti-apoptotic proteins as a final attempt to avoid cell death. Interestingly, the expression of the eIF4G-1 homolog, p97, which uses an IRES to initiate synthesis cap-independently, did show substantial change in abundance in these cells. Across each cell line the levels of p97 varied noticeably indicating IRES activity must be taken into account when considering overall protein synthesis in cells. Upon treatment with the chemotherapy drugs a substantial and reproducible decrease in p97 was seen, suggesting a shift in initiation mechanisms within the cell. A novel method for observing cap-dependent versus cap-independent translation initiation in the cell was developed using a dual-fluorescence reporter plasmid, and this system initially tested for EMCV IRES activity (and lack of IRES activity by other inserts) in breast cancer cell lines. Initial transfections with these plasmids has shown they have the ability to detect IRES activity in a single, live cell which can then be analyzed on an individual basis, or by cell populations.

Future directions should include developing a more effective means of treating cells with the chemotherapy drugs, while maintaining their viability for fluorescent reporter transfection. Such experiments would allow the eIF4G and p97 isoform representation profile to be established and correlated to the prevailing cap-dependent and –independent protein synthesis activity in live cells in real time. This could be combined with depletion of individual isoforms of eIF4G-1 to attempt to make correlations between specific isoforms and their role in apoptosis.

Further development of the dual fluorescence reporter plasmid to incorporate additional applications is also necessary. Method development for inducing and monitoring the IRES using chemotherapy drugs is an obvious next step. Experiments might also be developed to reverse the effects of the apoptosis-inducing drugs by beginning with cells in an apoptotic state indicated by IRES activity, and monitor the reduction in IRES use as cells recover following drug removal. The dual fluorescence plasmid can also be used in eIF4G-1 knockdown studies to explore the induction of IRES activity. Previous studies in the Keiper lab used a bicistronic reporter plasmid in whole populations of MCF7 cells and observed an induction of the Apaf-1 IRES of at least 5 fold when compared to the control in cells depleted of total eIF4G-1 indicating a shift in translation initiation mechanism (Blackwell 2007). Carrying out this experiment with the dual fluorescence live, single cell experiments would be very informative. By drawing correlations between eIF4G-1 isoforms, and the predominant mode of translation initiation being used on a single cell basis, cancerous cells could be targeted for cell death with greater insight into the actual physiological changes in protein synthesis. Defining eIF4G-1 isoforms as an apoptotic target could lead to lower effective doses of chemotherapy drugs, and an effective means of cancer inhibition with fewer side effects to patients.

References:

Alderden, R. A., M. D. Hall, et al. (2006). "The Discovery and Development of Cisplatin." Journal of Chemical Education 83(5): 728.

Blackwell, A. R. (2007). Effects of siRNA knockdown of translation initiation factor 4G-1 (eIF4G-1) isoforms in MCF7 breast cancer cells. Department of Biology. Greenville, East Carolina University.

Blanc, C. l., Q. L. Deveraux, et al. (2000). "Caspase-3 Is Essential for Procaspase-9 Processing and Cisplatin-induced Apoptosis of MCF-7 Breast Cancer Cells " Cancer Research 60 (16): 4386-4390

Bochkov, Y. A. and A. C. Palmenberg (2006). "Translational efficiency of EMCV IRES in bicistronic vectors is dependent upon IRES sequence and gene location." Biotechniques 41(3): 283-4, 286, 288 passim.

Bonneau, A. M. and N. Sonenberg (1987). "Proteolysis of the p220 component of the cap-binding protein complex is not sufficient for complete inhibition of host cell protein synthesis after poliovirus infection. ." Journal of Virology 61 (4): 986-991

Bradley, C., J. Padovan, et al. (2002). "Mass spectrometric analysis of the N terminus of translational initiation factor eIF4G-1 reveals novel isoforms." J Biol Chem 277(15): 12559-71.

Byrd, M., M. Zamora, et al. (2002). "Generation of multiple isoforms of eukaryotic translation initiation factor 4GI by use of alternate translation initiation codons." Mol Cell Biol 22(13): 4499-511.

Byrd, M., M. Zamora, et al. (2005). "Translation of eukaryotic translation initiation factor 4GI (eIF4GI) proceeds from multiple mRNAs containing a novel cap-dependent internal ribosome entry site (IRES) that is active during poliovirus infection." J Biol Chem 280(19): 18610-22.

Coldwell, M. and S. Morley (2006). "Specific isoforms of translation initiation factor 4GI show differences in translational activity." Mol Cell Biol 26(22): 8448-60.

Contreras, V., M. A. Richardson, et al. (2008). "Depletion of the cap-associated isoform of translation factor eIF4G induces germline apoptosis in C. elegans." Cell Death Differ 15(8): 1232-1242.

Cox, E., G. Burton, et al. (1989). "Cisplatin and etoposide: an effective treatment for refractory breast carcinoma." Am J Clin Oncol 12(1): 53-6.

De Benedetti, A. and J. Graff (2004). "eIF-4E expression and its role in malignancies and metastases." Oncogene 23(18): 3189-99.

Drevs, J., J. Fakler, et al. (2004). "Antiangiogenic Potency of Various Chemotherapeutic Drugs for Metronomic Chemotherapy." Anticancer Research 24(3A): 1759-1764.

Duriez, P. J. and G. M. Shah (1997). "Cleavage of poly(ADP-ribose) polymerase: a sensitive parameter to study cell death." Biochemistry and Cell Biology 75(4): 337-349.

Evan, G. I. and K. H. Vousden (2001). "Proliferation, cell cycle and apoptosis in cancer." 411(6835): 342-348.

Evans, D. and A. Howell (2007). Breast cancer risk-assessment models. Breast Cancer Research, BioMed Central. 9: 1-8.

Gradi, A., H. Imataka, et al. (1998). "A novel functional human eukaryotic translation initiation factor 4G." Mol Cell Biol 18(1): 334-42.

Henis-Korenblit, S., N. Strumpf, et al. (2000). "A novel form of DAP5 protein accumulates in apoptotic cells as a result of caspase cleavage and internal ribosome entry site-mediated translation." Mol Cell Biol 20(2): 496-506.

Holcik, M. and N. Sonenberg (2005). "Translational control in stress and apoptosis." 6(4): 318-327.

Holcik, M., N. Sonenberg, et al. (2000). "Internal ribosome initiation of translation and the control of cell death." Trends Genet 16(10): 469-73.

Houlbrook, S., C. M. Addison, et al. (1995). "Relationship between expression of topoisomerase II isoforms and intrinsic sensitivity to topoisomerase II inhibitors in breast cancer cell lines." Br J Cancer 72(6): 1454-61.

Imataka, H., H. Olsen, et al. (1997). "A new translational regulator with homology to eukaryotic translation initiation factor 4G." EMBO J 16(4): 817-25.

Jang, S., H. KrÃ¤usslich, et al. (1988). "A segment of the 5' nontranslated region of encephalomyocarditis virus RNA directs internal entry of ribosomes during in vitro translation." J Virol 62(8): 2636-43.

Janicke, R., M. Sprengart, et al. (1998). "Caspase-3 is required for DNA fragmentation and morphological changes associated with apoptosis." J Biol Chem 273(16): 9357-60.

Jemal, A., R. Siegel, et al. (2010). "Cancer Statistics, 2010." CA: A Cancer Journal for Clinicians 60(5): 277-300.

Joza, N., J. A. Pospisilik, et al. (2009). "AIF: Not Just an Apoptosis-Inducing Factor." Annals of the New York Academy of Sciences 1171(1): 2-11.

Keiper, B. and R. Rhoads (1997). "Cap-independent translation initiation in Xenopus oocytes." Nucleic Acids Res 25(2): 395-402.

Keiper, B. D., W. Gan, et al. (1999). "Protein synthesis initiation factor 4G." Int J Biochem Cell Biol 31(1): 37-41.

Komar, A. and M. Hatzoglou (2005). "Internal ribosome entry sites in cellular mRNAs: mystery of their existence." J Biol Chem 280(25): 23425-8.

Konecny, G. E., M. D. Pegram, et al. (2006). "Activity of the Dual Kinase Inhibitor Lapatinib (GW572016) against HER-2-Overexpressing and Trastuzumab-Treated Breast Cancer Cells" Cancer Research 66 (3): 1630-1639

Lowe, S. W. and A. W. Lin (2000). "Apoptosis in cancer" Carcinogenesis 21 (3): 485-495

Marissen, W. and R. Lloyd (1998). "Eukaryotic translation initiation factor 4G is targeted for proteolytic cleavage by caspase 3 during inhibition of translation in apoptotic cells." Mol Cell Biol 18(12): 7565-74.

Marissen, W. E., A. Gradi, et al. (2000). "Cleavage of eukaryotic translation initiation factor 4GII correlates with translation inhibition during apoptosis." Cell Death Differ 7(12): 1234-43.

Modjtahedi, N., F. Giordanetto, et al. (2006). "Apoptosis-inducing factor: vital and lethal." Trends Cell Biol 16(5): 264-72.

Morino, S., H. Imataka, et al. (2000). "Eukaryotic translation initiation factor 4E (eIF4E) binding site and the middle one-third of eIF4GI constitute the core domain for cap-dependent translation, and the C-terminal one-third functions as a modulatory region." Mol Cell Biol 20(2): 468-77.

Morley, S. J., M. J. Coldwell, et al. (2005). "Initiation factor modifications in the preapoptotic phase." Cell Death Differ 12(6): 571-584.

Morley, S. J., P. S. Curtis, et al. (1997). "eIF4G: translation's mystery factor begins to yield its secrets." Rna 3(10): 1085-104.

Nevins, T., Z. Harder, et al. (2003). "Distinct regulation of internal ribosome entry site-mediated translation following cellular stress is mediated by apoptotic fragments of eIF4G translation initiation factor family members eIF4GI and p97/DAP5/NAT1." J Biol Chem 278(6): 3572-9.

Nunez, G., M. Benedict, et al. (1998). "Caspases: the proteases of the apoptotic pathway." Oncogene 17(25): 3237-45.

Osborne, C. K. (1998). "Tamoxifen in the Treatment of Breast Cancer" New England Journal of Medicine 339(22): 1609-1618.

Prevot, D., J. Darlix, et al. (2003). "Conducting the initiation of protein synthesis: the role of eIF4G." Biol Cell 95(3-4): 141-56.

Schlotter, C. M., U. Vogt, et al. (2008). "Molecular targeted therapies for breast cancer treatment." Breast Cancer Res 10(4): 211.

Shapiro, C. L. and A. Recht (2001). "Side Effects of Adjuvant Treatment of Breast Cancer" New England Journal of Medicine 344(26): 1997-2008.

Sherrill, K. W., M. P. Byrd, et al. (2004). "BCL-2 Translation Is Mediated via Internal Ribosome Entry during Cell Stress" Journal of Biological Chemistry 279 (28): 29066-29074

Siddik, Z. H. (2003). "Cisplatin: mode of cytotoxic action and molecular basis of resistance." Oncogene 22(47): 7265-7279.

Vagner, S., B. Galy, et al. (2001). "Irresistible IRES. Attracting the translation machinery to internal ribosome entry sites." EMBO Rep 2(10): 893-8.

van Maanen, J. M. S., J. RetÃ¨l, et al. (1988). "Mechanism of Action of Antitumor Drug Etoposide: A Review " Journal of the National Cancer Institute 80 (19): 1526-1533

Vermeulen, K., D. R. Van Bockstaele, et al. (2003). "The cell cycle: a review of regulation, deregulation and therapeutic targets in cancer." Cell Proliferation 36(3): 131-149.

Vogel, C. L., M. A. Cobleigh, et al. (2002). "Efficacy and Safety of Trastuzumab as a Single Agent in First-Line Treatment of HER2-Overexpressing Metastatic Breast Cancer " Journal of Clinical Oncology 20 (3): 719-726

Yang, X.-H., T. L. Sladek, et al. (2001). "Reconstitution of Caspase 3 Sensitizes MCF-7 Breast Cancer Cells to Doxorubicin- and Etoposide-induced Apoptosis " Cancer Research 61 (1): 348-354